Continental Shelf Research 267 (2023) 105098

Contents lists available at ScienceDirect

Continental Shelf Research

journal homepage: www.elsevier.com/locate/csr

Modern conditions and recent environmental evolution of the industrialized inner Ría of Ferrol (Galicia, NW Spain)

Jon Gardoki [a,*], Alejandro Cearreta [a], María Jesús Irabien [a], José Gómez-Arozamena [b], Víctor Villasante-Marcos [c], Ane García-Artola [a], Carlos A. Galaz-Samaniego [d], María Cristina Peñalba [d], Filipa Bessa [e]

[a] Departamento de Geología, Facultad de Ciencia y Tecnología, Universidad del País Vasco UPV/EHU, Barrio Sarriena s/n, 48940, Leioa, Spain
[b] Departamento de Ciencias Médicas y Quirúrgicas, Facultad de Medicina, Universidad de Cantabria, Avenida Herrera Oria s/n, 39011, Santander, Spain
[c] Laboratorio de Magnetismo de Materiales y Magnetismo Ambiental, Instituto Geográfico Nacional, Real Observatorio de Madrid, C/Alfonso XII 3, 28014, Madrid, Spain
[d] Departamento de Investigaciones Científicas y Tecnológicas, Universidad de Sonora, Blvd. Luis Encinas y Rosales, 83000, Hermosillo, Sonora, Mexico
[e] University of Coimbra, MARE - Marine and Environmental Sciences Centre/ARNET – Aquatic Research Network, Department of Life Sciences, Calçada Martim de Freitas, 3000-456, Coimbra, Portugal

ARTICLE INFO

Keywords:
Benthic foraminifera
Trace metals
Pollen
Microplastics
Magnetic susceptibility
Ría of Ferrol

ABSTRACT

Galician rías provide several ecosystem services of great ecological and economic significance in the northwestern Iberian margin, requiring a good environmental quality for sustainable harnessing. More paleoenvironmental reconstructions extending to their preindustrial state are needed to predict their evolution under natural and human-induced perturbations, such as ongoing anthropogenic global warming. This study's aim is twofold: first, characterize the current environmental conditions governing the inner Ría of Ferrol (Galicia, NW Spain) and address its recent natural and anthropogenic evolution. Therefore, a multiproxy approach (benthic foraminifera, grain size, pollen content, trace metals, Al, total organic and inorganic carbon contents, total nitrogen content, $\delta^{13}C$, magnetic susceptibility, ^{210}Pb and ^{137}Cs radiotracers, and microplastics) has been applied to intertidal surface and sediment core samples. The benthic foraminiferal results exhibit typical inner ría assemblages, primarily driven by natural ría-estuarine dynamics, with a higher dominance of brackish species (*H. germanica*, *A.* morphogroup *tepida*), fewer living individuals and marine allochthonous taxa toward the continental end-member. The foraminiferal standing crops and surface trace metal concentrations do not reflect strong anthropogenic impacts, although areas with elevated magnetic susceptibility have been detected, probably associated with nearby industrial activities. The recent sedimentary deposits reveal anthropogenic impacts at local and regional scales, with different environmental shifts. Local impacts were triggered by physical interventions in the inner ría, with the construction of the As Pías Bridge in 1968 and the great urban-industrial development of Ferrol city and surrounding localities experienced since the late 19th century. Land-use changes have driven regional scale changes, corresponding to reforestation plans with the introduction of anthropogenic plant species for industrial purposes initiated in the 1940s. The stratigraphic analysis of sediment cores has unveiled high levels of contaminants (Zn and microplastics) in the innermost sector as the primary environmental concerns. In this sediment-infilling and restricted area, potential dredging activities could release them leading to their possible bioavailability. Although past adverse environmental conditions cannot be discarded, sedimentary intervals with negligible presence of microfauna in the innermost area have mostly been attributed to taphonomic processes involving calcareous dissolution and disaggregation of agglutinated tests, likely caused by carbonate-undersaturated conditions and organic matter metabolization by microbial activity respectively.

* Corresponding author.
E-mail address: jon.gardoqui@ehu.eus (J. Gardoki).

https://doi.org/10.1016/j.csr.2023.105098
Received 13 February 2023; Received in revised form 1 August 2023; Accepted 9 August 2023
Available online 21 August 2023

1. Introduction

Estuaries and similar coastal areas are highly dynamic and productive sedimentary environments providing numerous ecosystem services, such as nutrient regulation and coastal protection, and holding specialized biota, biological niches, commercially vital species, human settlements and tourism resources (Blythe et al., 2020; Newton et al., 2014). These partially enclosed coastal water bodies are typically subjected to the interplay of natural (salinity, temperature, turbidity and floods) and anthropogenic (land-use changes, urban, agricultural, industrial, and mining waste discharges) drivers. During the last decades, multiple human−driven interventions and ecological stressors have severely affected the estuaries (Garmendia et al., 2021; Teichert et al., 2016). Hence, their stability and functioning have deviated from their natural reference conditions (Borja and Dauer, 2008). These new conditions have left biological, chemical and physical imprints in the sedimentary record that can be compared with the original evidence (e.g., de Mora et al., 2004; Miranda and Yogui, 2016; Pan and Wang, 2012). Anthropogenic disturbances in coastal ecosystems can be detected using several signatures through the micropaleontological, sedimentological, and geochemical analyses of surface and core sediments (e.g., Alve, 1991; Pirrie et al., 2003; Vane et al., 2009). The multidisciplinary study of recent sedimentary records from coastal environments is an essential task under the current context of global warming, where these settings are already suffering severe ecological changes. These multiproxy analyses allow reconstruction of the environmental history and quality of such sensitive and vulnerable coastal systems through time and the different regional and/or global forcing mechanisms leading to their transformation. Furthermore, the comprehensive environmental and paleoecological reconstructions could provide local and regional authorities with a reference framework for future effective restoration and responsible coastal management (Borja et al., 2010).

The northwestern Atlantic Iberian coast, constituted by the Galician rías, comprises a sensitive and unique macroenvironment of significant ecological and socioeconomic value. The rías are long incised-valley embayments, with high surrounding reliefs and a characteristic funnel-shaped morphology, that extend over 1500 km along the coastline of the NW Iberian Peninsula (Evans and Prego, 2003; Mendez and Vilas, 2005). These depositional environments differ from typical estuaries by being strongly influenced by marine processes controlling the distribution of sedimentary facies, upwelling and downwelling events, water mixing, hydrodynamic circulation, and biogeochemical processes (e.g., deCastro et al., 2000; Diz et al., 2002; Ospina-Alvarez et al., 2010; Vilas et al., 2018). Furthermore, high biological productivity characterizes them, directly responding to upwelling phenomena that provide a significant nutrient supply for biomass production and, hence, supporting numerous ecosystem services and economic wealth to this region, such as mussel and clam drafts, fisheries, port activities, and tourism (Bode and Varela, 1998; Figueiras et al., 2002; Prego et al., 1999). Galicia is considered a critical fishing region within the European Union (Surís-Regueiro and Santiago, 2014). The urban settlements located at the margins of the rías (e.g., Ferrol, Vigo, A Coruña and Pontevedra), currently with more than 680,000 inhabitants, have experienced considerable development since the mid-20th century, primarily associated with industry, agriculture, mining, and livestock activities.

Studies have evidenced the potential of the Galician rías as a natural reservoir of several anthropogenic pollutants, such as trace metals, organic compounds and microplastics (Beiras et al., 2003a; Bellas et al., 2011; Carretero et al., 2021; Prego and Cobelo-García, 2003). In some cases, trace metals appear above the toxicological thresholds established by several sediment quality criteria (Álvarez-Iglesias et al., 2003; Beiras et al., 2003b; Bellas et al., 2008), and changes in redox conditions could release them into the water leading to their potential bioavailability to benthic micro- and macrofauna (Otero et al., 2005).

The Quaternary environmental transformation of the Galician rías has been extensively studied (e.g., Cartelle et al., 2022; Diz et al., 2002; García-Moreiras et al., 2019; Muñoz Sobrino et al., 2022), whereas other works have focused on the impact on biota by anthropogenic ecological stressors (Besada et al., 2002; Rial et al., 2017; Rodil et al., 2019). However, less attention has been paid to the transformation history of the rías during the last centuries (Álvarez-Iglesias et al., 2020; Álvarez-Vázquez et al., 2020; Cobelo-García and Prego, 2003) and a vital knowledge gap exists. In a global change context where Galician coastal areas are to experience severe disturbances, the recent environmental reconstructions based on geological evidence are critical to understanding and foreseeing future scenarios.

The Ría of Ferrol is a semi-enclosed embayment traditionally linked to the shipbuilding industry, where concentrations of trace metals in the sedimentary deposits have been successfully used as chemostratigraphic markers to assess the historical anthropogenic signature (Álvarez-Vázquez et al., 2020; Cobelo-García and Prego, 2003). This study addresses a wide multidisciplinary approach, including analyzing the benthic foraminifera, grain size, pollen content, trace metals (Pb, Zn, Cu and Ni), major element Al, elemental total nitrogen (TN), total organic carbon (TOC), total inorganic carbon (TIC), stable isotopes ($\delta^{13}C$), magnetic susceptibility, radionuclides (^{210}Pb, ^{137}Cs), and microplastics in surface and core samples from the inner ría. This study aims to provide a comprehensive and integrative view of the definite role played by human activities in the Ría of Ferrol, an excellent example of a coastal area with restricted conditions for water exchange with the nearby marine shelf. First, we have characterized the current environmental governing conditions to use them as modern analogs and assess the current quality state of this coastal area. Second, we have reconstructed the environmental transformation of the inner ría due to the interplay between local-regional natural and anthropogenic forcing mechanisms and identifying potential contaminants stored in the sediments.

2. Study area

The Ría of Ferrol (Galicia, northwestern Spain) and the Rías of Ares-Betanzos and A Coruña, known as part of the central Galician rías, comprise the Ártabro Gulf and drains its waters into the Atlantic Ocean. This mesotidal ría (1.5 m during neap tides to 4 m during spring tides) is 15 km long and 21 km^2 (deCastro et al., 2004). Its catchment basin, with an annual average rainfall of 1400 mm (Lueiro and Prego, 1999), lies on a Paleozoic basement constituted by abundant plutonic and metamorphic rocks, involving granites, gneisses, schists, slates and quartzites. Regarding vegetation, the catchment basin is part of the Eurosiberian Region, Cantabrian-Atlantic Province, and Galician-Asturian Sector (Izco, 1987). The natural vegetation is characterized by *Quercus robur* forests and *Alnus glutinosa* in the riversides, but extensive *Eucalyptus* and pine plantations materialize the strong human influence. Ferrol is a tide-dominated ría that, in contrast to the Rías Baixas of southern Galicia, stands out by its scarce upwelling influence (Prego and Varela, 1998). Its physiography, with a rock-bounded narrow channel, played a vital role during the postglacial transgression influencing the marine flooding that determined the distribution of depositional environments (Muñoz Sobrino et al., 2022). This ría can be divided into three primary parts: outer, middle and, inner sections (Fig. 1). The outer ría is the deepest (20–33 m deep) and presents a narrow channel close to the mouth complex. The morphology and bathymetry of the strait and the orientation of the primary ría axis, determine the ría-ocean exchange and favor well-mixed conditions in the narrow channel. However, the middle and inner areas are more stratified, particularly during wet seasons (Bode et al., 2005; deCastro et al., 2004; Varela et al., 2003). These middle and inner areas are shallower and more conditioned by the low freshwater inputs of the Xuvia and Belelle rivers (annual average of 6 and 0.8 $m^3\ s^{-1}$, respectively), favoring the stratification (deCastro et al., 2004). The middle ría, extending up to the As Pías Bridge (built in 1968), is 2 km long and <15

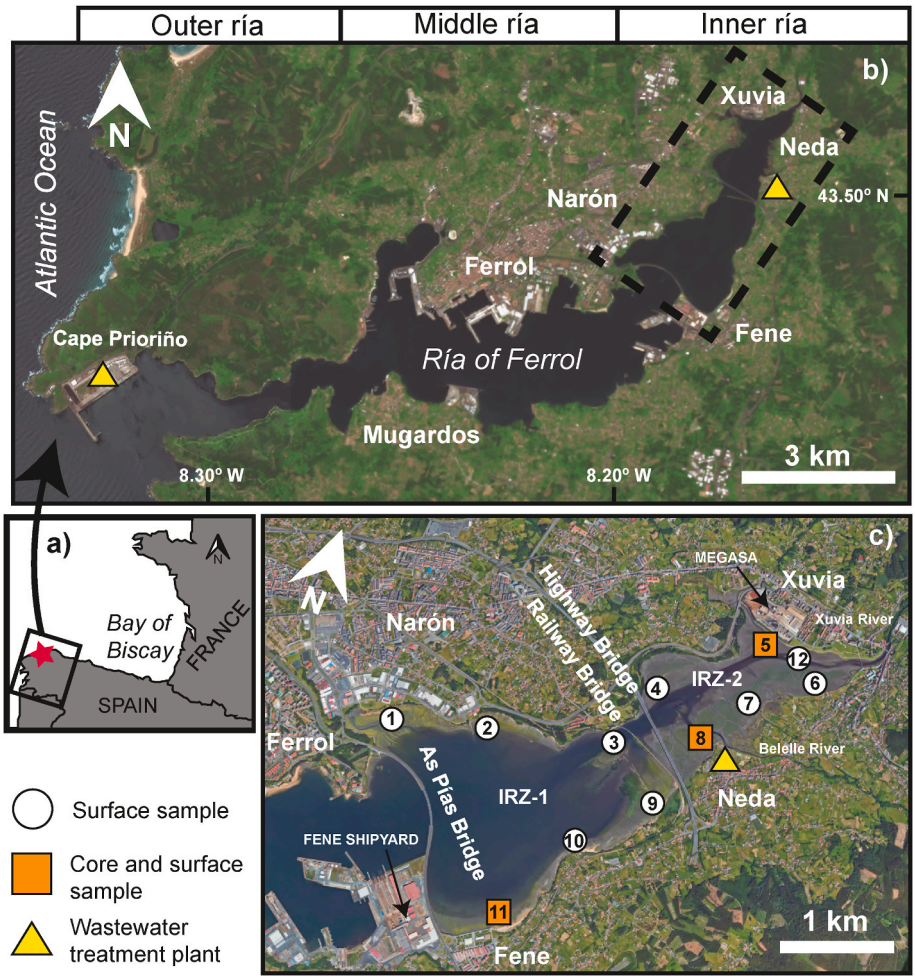

Fig. 1. Geographic location of the Ría of Ferrol in NW Spain (a), the localities mentioned in the text (b), and position of surface samples (white circles) and cores (orange squares) (c). For interpretation of the references to color in this figure legend, the reader is referred to the web version of the article.

m deep, whereas the innermost ría is very shallow, presents extensive intertidal mudflats, and is subdivided by two more bridges: the Railway (1913) and the Highway (2003).

Human occupation of the Ría of Ferrol margins started due to its excellent natural sheltered conditions and strategic position toward Europe and America for commercial maritime routes at least since the 14th and 15th centuries. From the 16th century onward, it became the Spanish Royal Navy official port and was fortified with arsenals and shipyards (Burgoa, 2020; O'Flanagan, 2008). In 1750, Ferrol became the most populated city of Galicia when the Esteiro Shipyards Military Arsenal was created (Burgoa, 2020; Martín García, 2001). However, they lost their importance with time. Around 1950, shipyard activities were reactivated, which along with the industrial development in the region, contributed to a critical demographic growth. The Ferrol, Fene, Mugardos, Narón and Neda localities evolved from 49,000 inhabitants in the early 20th century to more than 149,000 in the 1970s–1980s. With approximately 130,000 inhabitants, the most crucial industrial activities remaining are some shipyards, steel, metallurgical and chemical factories, and a petrochemical complex, all located in the middle and inner areas. The urban effluents in Ferrol and surrounding localities are chemically and biologically treated in two wastewater treatment plants at the outer part of the ría and in Neda (Fig. 1).

3. Material and methods

Twelve surface samples from different locations at the inner Ría of Ferrol were collected in May 2021 (3) and October 2022 (9) to study the modern foraminiferal assemblages (Fig. 1). To avoid patchiness at the microscale distribution of foraminifera and allow a quantitative study, two 1−cm thick replicates of 40 cm^2 (80 $cm^2 \times 1$ cm = 80 cm^3) at each sampling station were obtained by pressing a hard-plastic ring into the sediment (Murray and Alve, 2000). The sediment was placed in a plastic jar containing ethanol to prevent the foraminiferal protoplasm decay (Murray, 2006). At each sampling point, surface samples for granulometry, geochemical (trace metals, Al, TOC, TIC) and environmental magnetism (magnetic susceptibility) were collected by scraping the sediment uppermost millimeters with a plastic spatula. Moreover, three intertidal sediment cores were drilled in May 2021 from the inner Ría of Ferrol (Fene, Neda, and Xuvia cores). At each location, three 50−cm−long replicates of 11.5 cm in diameter were extracted (Fig. 1: Fene, Neda and Xuvia). Micropaleontological (benthic foraminifera and pollen content), grain size and geochemical studies (trace metals, Al, TOC and TIC contents, TN content, and carbon stable isotopes) were performed on one replicate, whereas the second and third replicates were used for radiometric and environmental magnetism analyses, respectively. In the innermost sampling location (Xuvia), an additional replicate core was extracted for microplastic analysis. All core replicates were divided into 1−cm intervals. Benthic foraminiferal, grain size, geochemical, and microplastic analyses were performed on alternate samples starting from 0-1 cm to 49–50 cm depth, except where changes were detected in the foraminiferal assemblages, in which case the intermediate sample was studied to provide maximum resolution. Radionuclide activity and magnetic susceptibility were measured at a 1-cm resolution.

Surface and core samples for foraminiferal and grain size analyses were washed through a 2 mm mesh to remove larger clasts and organic fragments and a 63 μm sieve to remove clay and silt fractions. After washing, a 1-g/L solution of Rose Bengal was added to the surface samples and left for an hour to distinguish alive individuals from dead tests (Walton, 1952). Subsequently, the surface and core samples were dried at 40 °C, and the foraminiferal tests were concentrated by flotation in trichloroethylene (Murray, 2006). The dry sandy residue containing the foraminifera was poured through a microsplitter (Murray, 2006) and studied under a stereoscopic binocular microscope using reflected light to identify different assemblages (alive, dead, and buried). A minimum of 300 foraminiferal tests per sample were extracted. When foraminifera were scarce, all the available tests were obtained and studied. Abundance results were expressed as a relative percentage of the total number of tests counted in each sample. The densities of living and dead foraminiferal assemblages from the surface samples are referred as the total number of individuals or tests/80 cm^3, respectively. The buried assemblage abundance from the cores was expressed as the number of individuals per 15 g of bulk dried sediment following García-Artola et al. (2016). In total, 111 samples and more than 22,000 benthic foraminifera were studied at the University of the Basque Country UPV/EHU (Spain) and taxonomically classified following Murray (1979), and Loeblich and Tappan (1988) and updated based on the World Register of Marine Species (WoRMS). Sixty-eight taxa were identified (Table A1), although

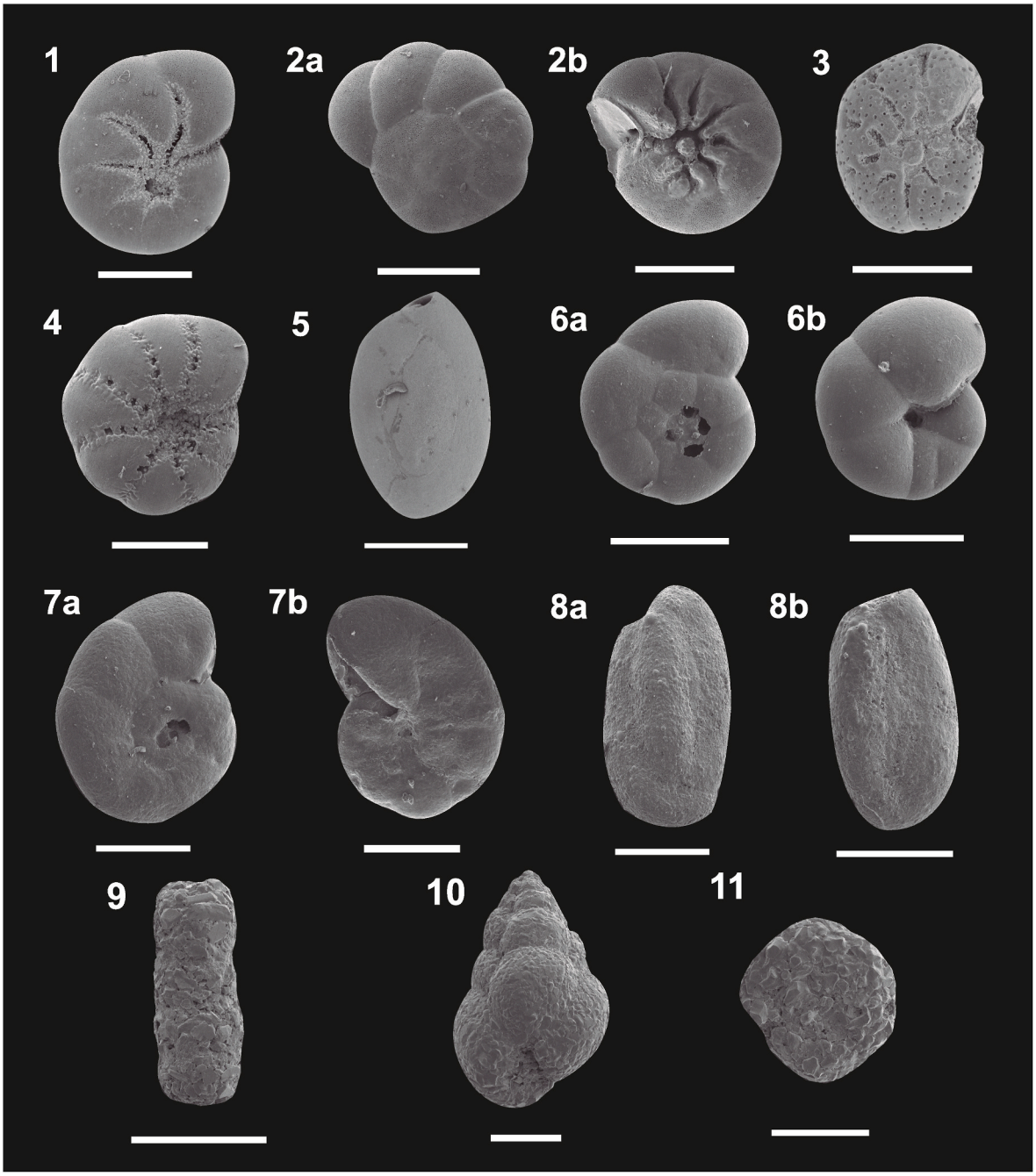

Fig. 2. SEM images of the main benthic foraminiferal species found in the inner Ría of Ferrol. 1 *Haynesina germanica* (Ehrenberg). 2 a,b *Ammonia* morphogroup *tepida* (Cushman). 3 *Elphidium oceanense* (d'Orbigny in Fornasini). 4 *Elphidium excavatum* (Terquem). 5 *Quinqueloculina seminulum* (Linnaeus). 6 a,b *Trochammina inflata* (Montagu). 7 a,b *Entzia macrescens* (Brady). 8 a,b *Miliammina fusca* (Brady), 9 *Scherochorella moniliformis* (Siddall). 10 *Eggerelloides scabrum* (Williamson). 11. *Ammoscalaria runiana* (Heron-Allen & Earland). Scale bar represents 100 μm.

only 18 species represented more than 2% in at least one sample. Scanning electron microscopy images of the principal species mentioned in the text (Fig. 2) and for the taphonomic characterization of the tests were obtained at the Analytical and High-resolution Microscopy in Biomedicine Service (SGIker, UPV/EHU/ERDT, EU). The environmental requirements for the foraminiferal species were primarily based on Cearreta (1988), Murray (2006), and Scott et al. (2007). Moreover, the assemblages were compared with available studies on living, dead and buried benthic foraminifera from the Ría of Ferrol (Mosquera Santé, 2000; Planelles de Miguel, 1996) and other nearby Galician rías (e.g., Alejo et al., 1999; Diz et al., 2004; Diz and Francés, 2008; Lebreiro et al., 2006; Mateu, 1987; Van Voorthuysen, 1973). Those species whose tests are primarily transported by hydrodynamic currents from the open sea shelf, outer sectors or subtidal environments of the ría were considered allochthonous taxa. Diagrams were created using Tilia version 2.6.1. The surface samples were statistically grouped using CONISS clustering (Grimm, 1987) after the normalization of the database by the square root transformation method. Sampling station 8 was excluded from the CONISS analysis since it yielded less than 100 tests/individuals. The percentage of mud (<63 μm), sand (63 μm–2 mm), and gravel (>2 mm) in each sample was calculated by weighing the dry residue retained in the 63 μm and 2 mm meshes. The results were expressed as percentages of bulk dried weight sediment.

The chemical treatment for the pollen extraction from the sediment was conducted following the modification proposed by Santos and Ledru (2021) based on using deflocculants and dense liquids for palynomorph extraction. *Lycopodium clavatum* spore tablets with a known concentration (for estimating the absolute pollen content in the sediment) were added to each sample previously soaked for 24 h and treated with HCl for carbonate removal. Subsequently, a concentrated detergent was added at a high temperature and left to stand for 24 h. The samples were again heated to temperatures close to the boiling point, and sodium hexametaphosphate was added to deflocculate the sediment and facilitate the separation of the organic from inorganic components through a 250 μm sieve and using a dense liquid (sodium polytungstate, 1.95 g cm^{-3}). The pollen extraction procedure was performed at the Laboratori d'Anàlisis Palinològiques of the Autonomous University of Barcelona, Spain.

The residues were stored in glycerin and analyzed by conventional optical microscopy at 400 × (Nikon Eclipse E200 microscope) in the laboratory of Terrestrial Natural Resources at the University of Sonora, Mexico, using specialized literature as a reference for identifying pollen content (Reille, 1992; Moore et al., 1994). A minimum of 300 pollen grains were counted for each sample, except in samples with low pollen concentrations, where at least 100 pollen grains were counted per sample. Data are shown as percentages regarding the total sum of pollen grains and spores of pteridophytes, and as pollen grains per gram of sediment for absolute values. Pollen functional types were generated by summing the relative frequencies of the following taxa:

1) Heathland: *Arbutus, Calluna vulgaris, Daboecia cantabrica, Erica scoparia*, Ericaceae, *Pteridium aquilinum,* and *Pyrola*
2) Grassland: Apiaceae, Asteroideae, Cichorioideae, *Plantago,* and Poaceae
3) Riparian forest: *Alnus, Betula, Corylus, Dryopteris filix-mas, Fraxinus, Juglans, Osmunda regalis, Salix,* and *Sambucus*
4) Anthropogenic plants: *Ailanthus*, *Ambrosia*, *Carya*, Cerealia, *Citrus, Eucalyptus, Liquidambar, Myrtus, Olea europaea, Pinus, Plantago, Vicia, Rumex,* and *Tamarix*

For trace metal concentration (Pb, Zn, Cu, Ni) and Al analysis, 0.5 g (<2 mm fraction) was mechanically homogenized using an agate mortar and pestle. Elemental concentrations were analyzed in Activation Laboratories Ltd. (Actlabs, Ontario, Canada) by inductively coupled plasma–optical emission spectrometry after digesting each sample in aqua regia, a mixture of concentrated hydrochloric and nitric acids, for 2 h at 95 °C. The detection limits were 2 mg kg^{-1} for Pb and Zn, 1 mg kg^{-1} for Cu and Ni and 0.01% for Al. For quality assurance and control, the digestion was 15% for each bath, two method reagent blanks, six in-house controls and four sample duplicates, and five certified reference materials. Data are represented normalized for Al concentrations (e.g., Zn/Al) to account for natural variation in granulometric and mineralogical compositions.

The analyses of TOC, TIC and TN of surface and core samples were performed using a LECO CNS 928 analyzer at the Scientific and Technique Soil Analysis Service from the Pyrenean Ecology Institute (IPE-CSIC, Zaragoza, Spain). The TOC is obtained by the difference between the total carbon (TC) and the TIC. For the TC analysis, 100 mg of dry sediment was mechanically homogenized using an agate mortar. Then, each sample was placed in small zirconia ceramic vessels at the laboratory and dried at approximately 1450 °C. The gases obtained by combustion passed through specific filters and a cooler, and later, they were mixed and reached equilibrium in a ballast at a known pressure. Subsequently, the gases were introduced within a stream of inert gas (He) and passed into a loop. Finally, the analyzer measured the loops to obtain the TC and TN. For the TIC analysis, 100 mg of homogenized sediment was dried at 360 °C for 4 h to eliminate the organic matter and analyzed with the LECO 928 analyzer. Carbon isotope ratios were determined in core sediment samples after eliminating of the inorganic carbon using an HCl 10% dissolution at Servizos de Apoio a Investigación (University of A Coruña, Spain). Capsulated samples were analyzed using a FlashEA1112 (ThermoFinnigan) elemental analyzer and a DeltaV Advantage (Thermo Scientific) isotope ratio mass spectrometer. The ratios were expressed as $\delta^{13}C$, where $[(R_{sample} - R_{standard})/R_{standard}] \times 1000$ and reported relative to the Vienna Pee Dee Belemnite standard.

Several natural (^{210}Pb and ^{226}Ra) and artificial (^{137}Cs) radiotracers were used to indicate the recent sedimentation processes. Moreover, sediment layer dating was performed by analyzing the vertical distribution of these radionuclide activities. ^{210}Pb, ^{226}Ra, and ^{137}Cs were determined by gamma spectrometry in samples from cores using an HPGe detector at the University of Cantabria, Spain. The analytical procedures used have been discussed in former contributions (Cearreta et al., 2013; Irabien et al., 2008).

Low-frequency, mass–normalized bulk magnetic susceptibility (χ, $m^3\ kg^{-1}$) was measured 10 times for each sample with Bartington MS3/MS2B equipment after being dried at 40 °C at the L-MAGMA (National Geographic Institute, Madrid, Spain). The average values and standard deviations (1σ) were calculated and presented.

Microplastic extraction was performed in a clean and restricted laboratory room to avoid airborne fiber contamination, using the methodology adapted from Frias et al. (2018). The sediment samples were weighed after drying in an oven at 50 °C for 48 h. The samples were placed in 1 L glass beakers where 150 ml of 20% hydrogen peroxide was added to reduce the organic matter in the sediments (24 h at room temperature). Each sample was subsequently poured into a 500 μm sieve (the lower limit of detection used in this study) using filtered distilled water. The >500 μm fraction of each sample was then transferred to a glass beaker containing a supersaturated saline solution (NaCl, 1.2 g cm^{-3}), where potential microplastics floated and were allowed to settle for 2 h. Finally, the supernatant was vacuum filtered through 1.2 μm Whatman GF/C microfiber filter papers, and the filters were sealed in a Petri dish before the stereomicroscope analysis. As airborne contamination control, a glass fiber in a Petri dish was left open in the laboratory during the entire sample processing before being examined under the microscope as above. Four blue fibers were observed, suggesting that sample contamination during processing, and while uncovered it is approximately 0.08 fiber h^{-1}. All suspected particles were extracted from the filters and characterized according to shape (i.e., fiber, film fragment, pellet, or fiber bundle) and color and measured at their largest cross-section (mm) under a dissecting microscope coupled with an image analysis system IC80 HD Camera with Leica Application Suite

software. Careful criteria were used for visual identifying microplastics, and only larger particles were included in this study (500–5000 μm total length). The particles with homogenous thicknesses across their lengths, a homogenous colors and gloss were not selected. Furthermore, the hot-needle test was performed by heating the tip of a thin needle and poking a suspected microplastic under the stereomicroscope (De Witte et al., 2014). In total, 290 microplastics were identified from direct microscopic analysis of the sediment samples at the University of Coimbra, Portugal. The particle concentrations on a number basis were normalized to the dry sediment mass (the number of particles per kg of dry-weight sediment).

4. Results and discussion

4.1. Surface samples

Living benthic foraminifera respond to different environmental parameters (e.g., salinity, sediment grain size, nutrients, oxygen and temperature) by changing their abundances and specific compositions. In turn, dead foraminiferal assemblages present a cumulative character since they are formed by the recent production of successive populations and transported foraminifera within a short period (Murray, 2006).

Based on the CONISS analysis of the living and dead foraminiferal contents, two primary sectors can be distinguished along the inner Ría of Ferrol: The inner Ría Zone 1 (IRZ-1) and the inner Ría Zone 2 (IRZ-2) (Fig. 3). The IRZ-1, from the As Pías Bridge to the Railway Bridge (Fig. 1), presents very high numbers of live and dead foraminifera (ranges: 240–5858 individuals/80 cm^3 and 322–6198 tests/80 cm^3, respectively), an average of 42% dead marine taxa (allochthonous) and a variable mud (average 65%), sand (33%), and gravel (2%) contents (Fig. 3). The living assemblages primarily comprised hyaline tests, with *Haynesina germanica* (46%) and *Ammonia* morphogroup *tepida* (32%) as the primary species. *Quinqueloculina seminulum* (8%) and *Elphidium oceanense* (6%) appeared as secondary taxa. This living assemblage contained autochthonous taxa, indicating brackish conditions, typically found in the northern Iberian coast estuaries and inner rías (Cearreta and Murray, 1996; Diz and Francés, 2008; Mateu, 1987; Pascual et al., 2019; Rodríguez-Lázaro et al., 2013). *Haynesina germanica* and *A.* morphogroup *tepida* are euryhaline species that can be found inhabiting estuarine muddy and silty tidal flats under variable and relatively low salinity conditions (Horton and Murray, 2007). However, the presence of *Q. seminulum* and *E. oceanense* in the biocoenosis suggests a higher salinity range (Murray, 2006) (Table 1). On the other hand, *Eggerelloides scabrum* (average 34%), *H. germanica* (29%) and *A.* morphogroup *tepida* (18%) appeared as dominant species in the dead assemblages, with porcellaneous taxa such as *Q. seminulum* constituting ~5%. High percentages of hyaline and agglutinated tests dominate the assemblage (Table 2). While most of the calcareous taxa are roughly pristine (Fig. 4

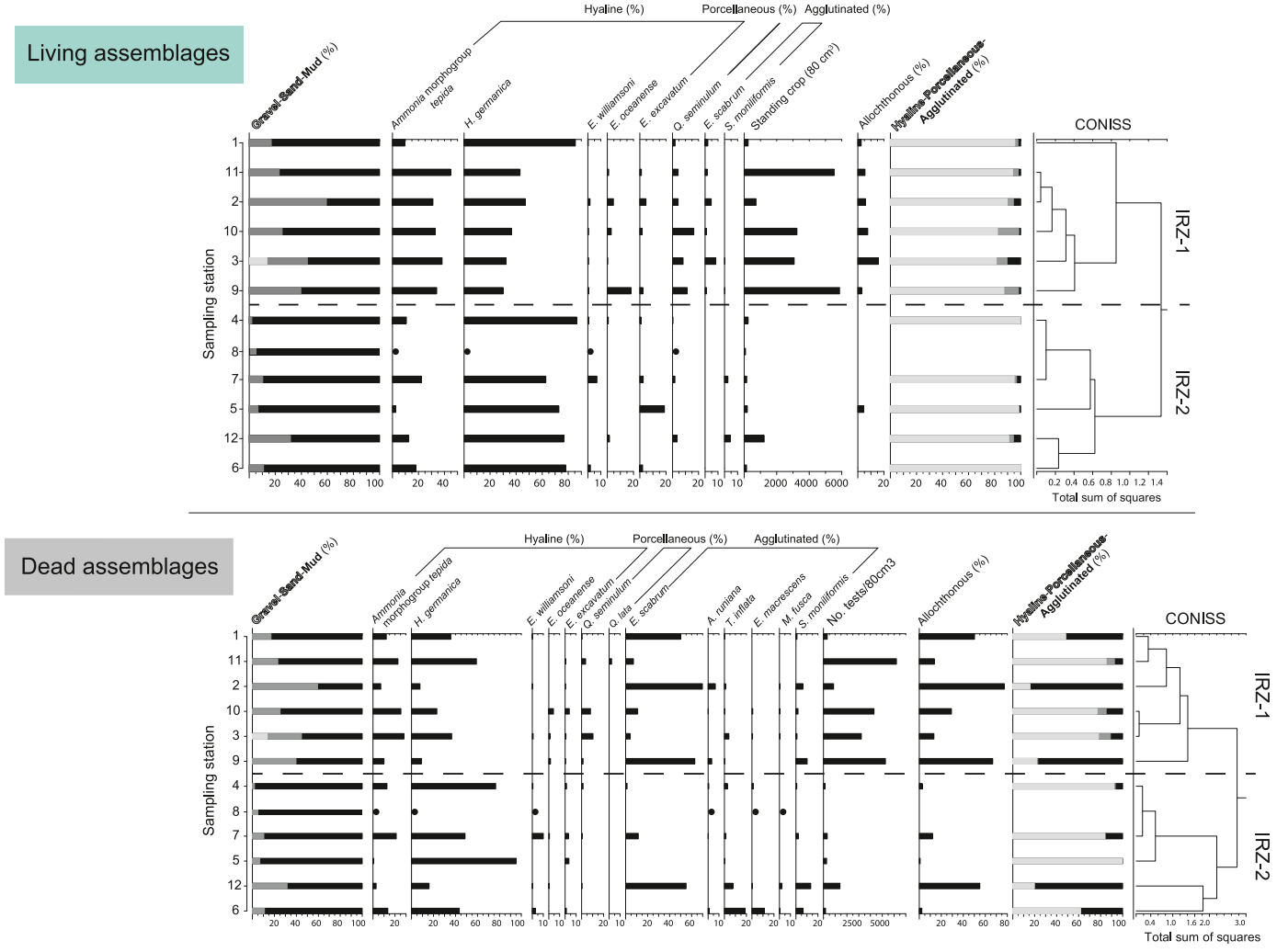

Fig. 3. Distribution of grain-size contents (%) and relative abundance of main foraminiferal species in the living and dead assemblages (%) along the surface sample stations from the inner Ría of Ferrol. Note that sampling station 8 is excluded from the CONISS analysis, since it yielded less than <100 tests/individuals. Black dots represent samples with <100 tests.

Table 1
Ecological preferences of the most characteristic benthic foraminiferal species found in the inner Ría of Ferrol.

Species	Ecological preferences
***Haynesina germanica* (Ehrenberg)**	It is a hyaline species typically living in intertidal mudflats and subtidal environments with different salinity levels. It is an euryhaline taxon that can be found in transitional ecosystems associated to silty and fine-sandy sediments with highly variable TOC (Alve and Murray, 1999; Murray, 2006). It has been found in estuaries with severe trace metals pollution along with *Ammonia* group species and *E. oceanense* (Cearreta et al., 2000).
***Ammonia* morphogroup *tepida* (Cushman)**	It is a group of hyaline forms found in intertidal and subtidal estuarine areas, low marshes and hypersaline lagoons (Murray, 2006). They have been described as an euryhaline and opportunistic species, living in sediments with variable mud and TOC contents (Murray, 2006).
***Elphidium oceanense* (d'Orbigny in Fornasini)**	It is a hyaline infaunal detritivore species, usually found in transitional environments, mostly intertidal and subtidal shallow areas (Alve and Murray, 1999; Murray, 2006).
***Elphidium excavatum* (Terquem)**	It is a hyaline species found in intertidal and subtidal estuarine environments, but also marine and lagoon areas, with variable sand and mud content (Alve and Murray, 1999; Murray, 2006). It has been described as a tolerant taxon to anthropogenic pollution (Scott et al., 2007).
***Quinqueloculina seminulum* (Linnaeus)**	It is a porcellaneous epifaunal and infaunal taxon characteristic of lower estuary, inner shelf, normal marine lagoons and low marsh environments (Jorissen, 1987; Murray, 2006).
***Eggerelloides scabrum* (Williamson)**	It is an agglutinated widely distributed infaunal species, usually found under subtidal conditions along open-sea shelf environments and fjords, also extending into shallow waters with high energy and marginal coastal areas, particularly in the mouth of the estuaries (Dessandier et al., 2015; Jorissen et al., 1992; Mojtahid et al., 2008; Murray and Alve 1999a). It presents a wide range of grain size selection (Scott et al., 1998). This taxon does not seem to have a substrate dependence nor labile organic matter preference, feeding on different nutrient sources (Diz et al., 2006). It is an excellent competitor for space and nutrients, also capable of thriving under highly variable environmental conditions, ranging from well oxygenated waters to nearly hypoxia (Cesbron et al., 2016; Diz et al., 2006; Fontanier et al., 2022).
***Ammoscalaria runiana* (Heron-Allen & Earland)**	It is an agglutinated species usually found in marine and coastal environments with fine to coarse-grained sediments and low TOC (Alve and Murray, 1999; Murray, 2006). It presents a very wide range of grain size selection (Scott et al., 1998).
***Miliammina fusca* (Brady)**	It is an agglutinated miliolid usually found in intertidal flats to low marshes (Horton et al., 1999). Although it is described as an euryhaline species, it is more frequent in hyposaline areas (Alve and Murray, 1999). This taxon inhabits the continental end member environments highly influenced by the freshwater input (Debenay et al., 2002).
***Scherochorella moniliformis* (Siddall)**	It is an agglutinated taxon found in intertidal flats to low marsh environments, probably feeding on plant debris (Alve and Murray, 1999; Avnaim-Katav et al., 2017).
***Trochammina inflata* (Montagu)**	It is an euryhaline agglutinated species typically living in low to high vegetated marsh environments (Horton et al., 1999; Murray, 2006).
***Entzia macrescens* (Brady)**	It is an euryhaline agglutinated species living in low to high vegetated marsh environments (Horton et al., 1999; Horton and Murray, 2007; Murray, 2006). It is more frequent in mid-high marshes (de Rijk and Troelstra, 1997; Scott et al., 2007).

Table 2
Summary of sedimentological and micropaleontological data from surface samples collected along the inner Ría of Ferrol. The single value represents the average and those in parentheses the range.

	Living assemblages	Dead assemblages
IRZ-1		
Mud 65 (41–83) %		
Sand 33 (17–60) %		
Gravel 2 (0–13) %		
No. Tests/80 cm^3	3114 (250–5858)	3361 (322–6198)
Marine tests %	7 (3–16)	42 (13–77)
Hyaline %	88 (81–95)	54 (16–85)
Porcellaneous %	8 (3–16)	5 (0–11)
Agglutinated %	4 (2–11)	41 (7–84)
Linings/sample	0	7 (1–13)
E. scabrum %	3 (1–8)	34 (4–70)
H. germanica %	32 (10–45)	29 (8–60)
A. morphogroup *tepida* %	46 (30–85)	18 (7–28)
Q. seminulum %	8 (2–16)	4 (0–10)
E. oceanense %	6 (0–18)	1 (0–4)
IRZ-2		
Mud 89 (68–98) %		
Sand 11 (2–32) %		
No. Tests/80 cm^3	338 (34–1230)	396 (18–1412)
Marine tests %	1 (0–5)	15 (1–55)
Hyaline %	97 (91–100)	71 (20–100)
Porcellaneous %	1 (0–4)	0.4 (0–1)
Agglutinated %	2 (0–6)	28 (0–80)
Linings/sample	0	5 (0–12)
H. germanica %	75 (63–87)	56 (16–95)
A. morphogroup *tepida* %	13 (3–22)	10 (0–21)
E. scabrum %	0	14 (0–55)
E. excavatum %	6 (0–19)	0
T. inflata %	0.1 (0–0.6)	6 (0–19)
S. moniliformis %	1.4 (0–4.3)	5 (0–14)
E. macrescens %	0	3 (0–11)

a, b), some dead hyaline tests show partial dissolution with the exposure of the inner organic lining (Fig. 4 c, d), ranging from 1 to 13 linings/sample.

A similar dead assemblage to that observed in IRZ-1, primarily comprising *H. germanica*, *A.* morphogroup *tepida,* and *E. scabrum*, was also found in the sandy subtidal sediments from the Ría of Vigo innermost area (southern Galicia), but with lower proportions of *E. scabrum* (Diz and Francés, 2008). The very low abundances of this taxon in the living assemblages of IRZ-1 (3%), compared to its high percentages in the thanatocoenosis (Table 2), indicate that *E. scabrum* might not find adequate environmental conditions to develop and that tidal currents transport a great proportion of its dead tests from the outer and/or subtidal areas of this ría (Table 1). In the Galician rías, it was found in the outer and inner areas living in muddy and fine-sandy sediments, typically with elevated organic matter contents (Alejo et al., 1999; Diz and Francés, 2008; Mateu, 1987).

The exposure of organic linings related to thin calcareous tests (Fig. 4 c) denotes *post-mortem* dissolution occurring at the topmost centimeter of the sediment surface due to severe calcium carbonate-undersaturated conditions (Moreno et al., 2007), as expressed by the low TIC contents (Table 3). Diz and Francés (2009), in the nearby Ría of Vigo, invoked dissolution processes affecting the preservation of calcareous taxa. This taphonomic phenomenon could partially result from a corrosive burial environment, since the catchment basin primarily comprises

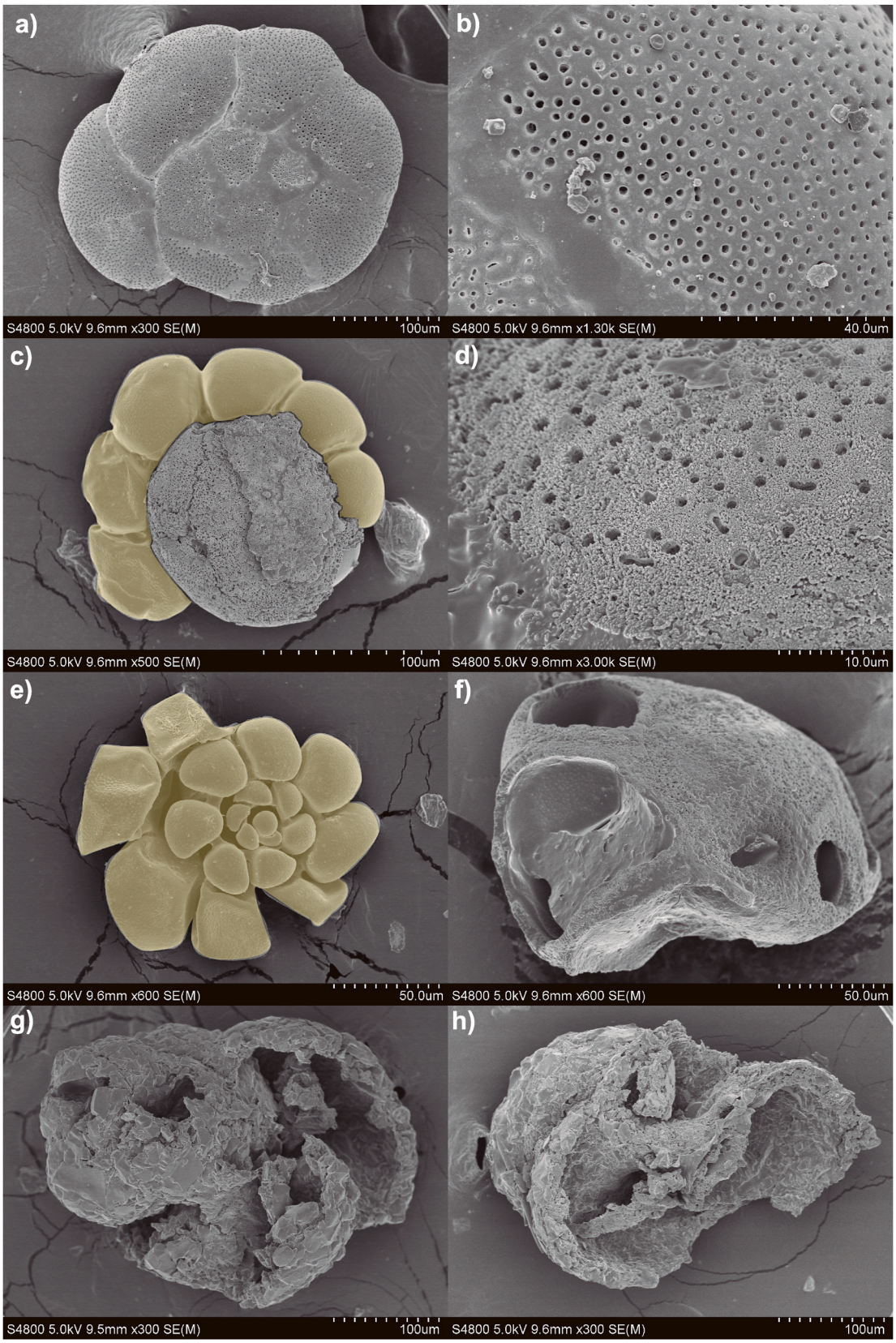

Fig. 4. Pristine dorsal view of calcareous *Ammonia* morphogroup *tepida* from the Ría of Ferrol (a) and test surface texture (b) under the scanning electron microscope. Dissolved test of *A.* morphogroup *tepida* with the partial exposure of the inner organic lining (c). Irregular corroded surface texture of *A.* morphogroup *tepida* (d). Exposure of inner organic linings of *A.* morphogroup *tepida* (e). Dorsal view of *A.* morphogroup *tepida* with collapsed chambers (f). Wall fracturing and collapse of *Eggerelloides scabrum* tests (g) (h). Linings are artificially colored for identification.

Table 3
Range of concentrations in surface and core sediments from the inner Ría of Ferrol, values for northern Iberian estuaries and rías proposed by different authors, Sediment Quality Guidelines and Spanish classification of dredged materials. Trace metal values are expressed in mg kg^{-1}, TOC-TIC-TN contents and $\delta^{13}C$ in % and magnetic susceptibility (χ) values in 10^{-7} m^3 kg^{-1} (standard deviation < $0.05{\cdot}10^{-7}$ m^3 kg^{-1}). Microplastic density content is expressed in number of particles kg^{-1} dry weight sediment.

	Cu	Pb	Zn	Ni	TOC	TIC	TN	$\delta^{13}C$	χ	Microplastics
Inner Ría of Ferrol (This work)										
IRZ-1 (n=6)	21–58	14–34	72–148	10–21	0.8–2.4	0.06–0.19	0.13–0.31	–	0.73–1.51	–
IRZ-2 (n=5)[a]	67–95	44–47	163–264	29–34	3.8–6.2	0.03–0.11	0.39–0.62	–	1.39–2.74[b]	–
Fen-1 (n=24)	21–38	9–20	73–93	24–37	1.8–4.3	0.00–0.17	0.18–0.48	−20.6 to −18.4	0.73–0.85	–
Fen-2 (n=11)	26–73	14–39	85–206	20–27	1.9–2.5	0.00–0.24	0.18–0.34	−22.2 to −20.6	0.80–1.43	–
Ned-1 (n=4)	59–74	51–55	141–255	28–34	3.2–4.6	0.04–0.07	0.28–0.41	−23.3 to −22.6	0.76–0.81	–
Ned-2 (n=28)	80–103	44–56	163–328	31–37	4.8–6.2	0.00–0.06	0.40–0.62	−24.4 to −23.3	0.82–2.74	–
Xuv-1 (n=17)	34–152	34–165	87–667	33–51	1.8–5.2	0.05–0.3	0.12–0.44	−24.3 to −21.1	0.82–26.26	0–104
Xuv-2 (n=15)	77–143	45–150	248–598	29–55	4.1–5.2	0.03–0.13	0.35–0.45	−25.2 to −23.8	2.06–10.52	94–463
Industrialized Galician rías										
Vigo (Prego and Cobelo-García, 2003)	nd-140	0–5200	0–1160	0–101	–	–	–	–	–	–
A Coruña (Prego and Cobelo-García, 2003)	0–315	0–460	0–1300	0–44	–	–	–	–	–	–
Pontevedra (Carballeira et al., 1997)	58–355	116–332	220–697	33–45	–	–	–	–	–	–
Cantabrian coast estuaries										
Bilbao (Cearreta et al., 2000)	41–1946	75–2566	167–7687	20–129	–	–	–	–	–	–
Suances (Serrano, 2020)	26–104	544–2700	2070–10,000	11–28	–	–	–	–	–	–
Pasaia (Irabien et al., 2020)	7–4490	12- >5000	65- >10,000	12–175	–	–	–	–	–	–
Reference values										
ERM (Long et al., 1995)	270	218	410	51.6	–	–	–	–	–	–
Action Level B	168	218	410	63	–	–	–	–	–	–
Action Level C (Buceta et al., 2015)	675	600	1640	234	–	–	–	–	–	–
Background Ferrol (Cobelo-García and Prego, 2003)	12 ± 3	27 ± 5	55 ± 11	26 ± 10	–	–	–	–	–	–
Ares	25–33	28–34	109–149	24–32	–	–	–	–	–	–
Betanzos (Álvarez-Vázquez et al., 2017)	17–27	17–33	72–113	21–26	–	–	–	–	–	–
Galician estuaries (Carballeira et al., 2000)	20–35	50–78	120–136	31–38	–	–	–	–	–	–

[a] Except sample 12 (0.8% TOC, 0.14% TN, 152 mg kg^{-1}Zn, 23 mg kg^{-1}Pb, 31 mg kg^{-1}Cu, 18 mg kg^{-1}Ni).
[b] Except samples 5 and 12, that show values of 3.69 and $5.15{\cdot}10^{-7}m^3kg^{-1}$,respectively.

siliceous-rich igneous and metamorphic rocks, resulting in carbonate-undersaturated freshwater flowing into the innermost ría. Contrary to observations made by Buzas-Stephens and Buzas (2005) in the Nueces Bay (Texas), in Ferrol only the dead tests show dissolution-driven signals, but not the living specimens. Hence, calcareous dissolution is considered a *post-mortem* process, not inhibiting the development of stable living hyaline populations. Despite this taphonomic phenomenon, the assemblages from IRZ-1 correlate well with those recorded previously by Planelles de Miguel (1996) in the inner Ría of Ferrol and by Diz and Francés (2008) in similar areas from the Ría of Vigo, reflecting a brackish intertidal sandy-mudflat environment conditioned by the oceanic influx.

The IRZ-2 sector extends from the Railway Bridge to the Xuvia River (Fig. 1) and shows predominantly muddy sediments (>88%) with moderate foraminiferal densities (living: 150–1230 individuals/80 cm^3, dead: 150–1412 tests/80 cm^3), except for the very low numbers in sampling station 8 (34 living individuals/80 cm^3 and 18 dead tests/80 cm^3), and reduced abundances of dead marine taxa (15%) (Fig. 3). On the one hand, hyaline taxa (97%) dominate the biocoenosis, primarily *H. germanica* (75%) and *A.* morphogroup *tepida* (13%), with the secondary presence of *Elphidium excavatum* (6%). The high dominance of these species, and the overall muddy sediments and higher organic carbon contents (Table 3), indicate that IRZ-2 is a more confined environment, characterized by extensive mudflats with brackish hydrochemical conditions and a more restricted marine inflow. However, *H. germanica* (56%), *E. scabrum* (14%), and *A.* morphogroup *tepida* (10%) form thanatocoenosis as the principal taxa. It is noteworthy the presence of low-salinity agglutinated species (Table 1), such as *Trochammina inflata*, *Entzia macrescens*, *Miliammina fusca* and *Scherochorella moniliformis* that together compose up to an average 14% of the dead assemblage. The species abundances indicate the continental influence in this innermost area (Debenay et al., 2006). The number of partially-dissolved dead hyaline tests showing their lining is similar to that determined in the previous zone, since it ranges from 0 to 12 linings/sample.

Regarding the geochemical and magnetism results, muddy samples in IRZ-2 show higher concentrations of organic carbon, TN, and trace metals and higher susceptibility values than those observed in IRZ-1 (Table 3). This enrichment seems related to granulometric differences given the reasonably good correlations found between Al and Zn (0.76), Pb (0.88), Cu (0.86), and Ni (0.92) and to the paramagnetic character of the clay minerals (Evans and Heller, 2003) of the mud fraction. However, the sandier sediments from IRZ-1, with a quartz-rich mineral association, would have lower levels of trace metals and a stronger diamagnetic signal with lower magnetic susceptibility values. Sediments collected in sampling site 12 and, to a lesser extent in site 5, exhibit significantly higher values of magnetic susceptibility (Table 3; 5.15 and $3.69{\cdot}10^{-7}$ m^3 kg^{-1}, respectively). Both sites are adjacent to a steel plant

(Megasa Siderúrgica Narón; Fig. 1), likely to be the primary source of ferromagnetic particles in this area.

4.2. Fene core

Based on its micropaleontological content, geochemical, and physical features, two stratigraphic units or depth intervals can be distinguished in the Fene core (Fen-1 and Fen-2; Fig. 5). Basal Fen-1 (50-15 cm) is an overall muddy interval (average mud content 88%). It is characterized by the species *E. scabrum* (average 81%), *A.* morphogroup *tepida* (12%), and *H. germanica* (7%), with the secondary presence of *Ammoscalaria runiana* (2%). Foraminiferal densities show very low values at the base of the sequence that increase to moderate and high values in the upper part (range 12–367 tests/15 g). The data suggest the existence of an intertidal flat depositional environment strongly subjected to the oceanic influx (Diz and Francés, 2008). Moreover, the palynological analysis of the basal part of the sequence shows a low pollen concentration, possibly related to a greater marine influence, which can determine a greater distance from the vegetation source and might affect the preservation of pollen grains (Heusser and Stock, 1984). Pollen concentrations tend to be lower in the seaward locations of the estuaries and rías (Chmura, 1994; Ellison, 2017). Agglutinated and marine allochthonous taxa dominate the foraminiferal assemblages, representing an average percentage of approximately 83% (Table 4). As modern analogs, only salt marshes and ocean environments below the carbonate compensation depth present many agglutinated benthic foraminifera (Murray and Alve, 1999a); therefore, these values indicate an underlying taphonomic process. Hyaline tests show typical dissolution-driven characteristics, such as thin tests, loss of calcareous layers, irregular corroded surfaces, collapsed chambers, the exposure of inner organic linings, and, on numerous occasions, the only appearance of their linings, as observed under the scanning electron microscope (Fig. 4). The number of linings belonging to calcareous taxa in Fen-1 is high, reaching an average of 17 per sample. The relative abundances of agglutinated taxa, the observed taphonomic characteristics on calcareous tests, and the low inorganic carbon content (Table 3) indicate that *post-mortem* dissolution could represent a crucial driver (Moreno et al., 2007; Murray and Alve, 1999a, 1999b; Valente et al., 2009).

The vertical distribution of TOC and TN through Fen-1 reveals a slightly fluctuating pattern, with overall values similar to marine-influenced areas (Andrews et al., 2000; Meyers, 1997), also expressed by the $\delta^{13}C$ values (Mackie et al., 2005). However, the TIC contents remain near zero along this basal part of the core (Fig. 5). The trace metal concentrations are the lowest determined in this work (Table 3), and Al-normalized values display fairly constant profiles (Fig. 5). Likewise, magnetic susceptibility presents a rather homogeneous pattern and low values, highlighting the scarce presence of ferromagnetic minerals. Very high abundances of heathland- and grassland-type pollen

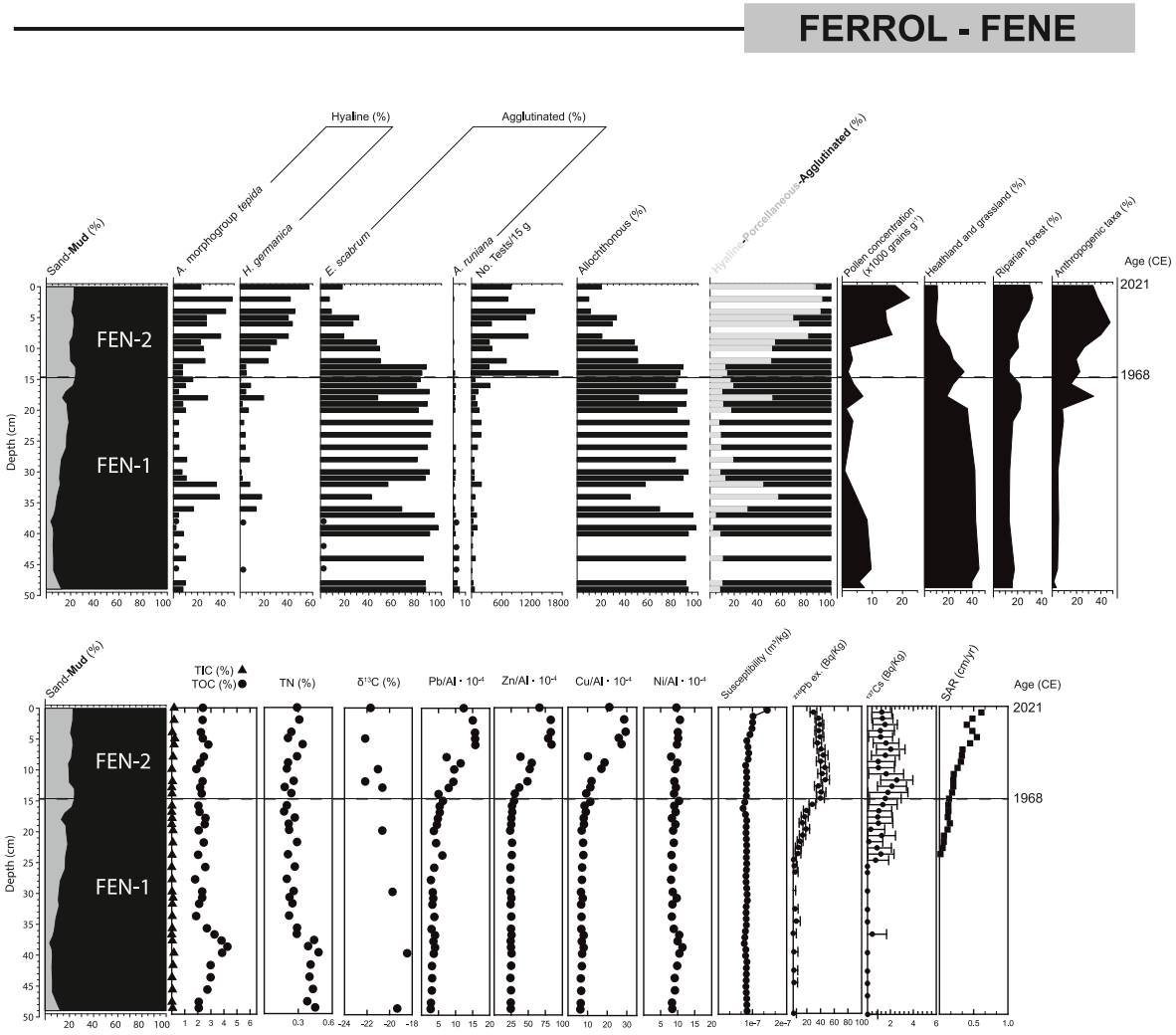

Fig. 5. Vertical distribution of grain-size contents (%), relative abundance of main foraminiferal species (%), pollen concentration (x1000 grain g^{-1} sediment), relative abundance of main Pollen Functional Types (%), TOC, TIC, TN and $\delta^{13}C$ (%), trace metals, magnetic susceptibility (m^3 kg^{-1}), $^{210}Pb_{xs}$ and ^{137}Cs activities (Bq kg^{-1}) and Sediment Accumulation Rate (cm yr^{-1}) in the Fene core, inner Ría of Ferrol. Black dots represent samples with <100 tests.

Table 4
Summary of sedimentological and micropaleontological data (foraminifera and pollen) from cores drilled in the inner Ría of Ferrol. The single value represents the average and those in parentheses the range.

Fene	
Fen-1 (50-15 cm)	Fen-2 (15-0 cm)
Mud 88 (76–94) %	Mud 78 (76–81) %
Sand 12 (4–24) %	Sand 22 (20–24)
No. Tests/15 g 95 (12–367)	No. Tests/15 g 801 (347–1718)
Marine 83 (44–98) %	Marine 40 (10–88) %
Hyaline 17 (2–56) %	Hyaline 61 (12–92) %
Agglutinated 83 (44–98) %	Agglutinated 39 (7–88) %
Linings/sample 17 (4–54)	Linings/sample 11 (1–29)
E. scabrum 81 (42–97) %	*E. scabrum* 39 (7–88) %
A. morphogroup *tepida* 12 (2–38) %	*H. germanica* 32 (5–59) %
H. germanica 7 (0–20) %	*A.* morphogroup *tepida* 27 (7–49) %
A. runiana 2 (0–5) %	
Pollen concentration 5309 (885–9640) grains/g	Pollen concentration 11,723 (2047–22,338) grains/g
Heathland – Grassland 36 (19–45) %	Heathland – Grassland 16 (10–33) %
Riparian forest 17 (13–23) %	Riparian forest 22 (12–32) %
Anthropogenic taxa 9 (1–34) %	Anthropogenic taxa 34 (19–48) %
Neda	
Ned-1 (50-46 cm)	Ned-2 (46-0 cm) (<100 tests/sample)
Mud 77 (72–83) %	Mud 94 (86–97) %
Sand 20 (11–26) %	Sand 6 (3–11) %
Gravel 3 (2–6) %	Gravel 0%
No. Tests/15 g 45 (31–53)	No. Tests/15 g 3 (0–14)
Marine 90 (84–97) %	Marine - %
Hyaline 7 (1–14) %	Hyaline - %
Agglutinated 93 (86–99) %	Agglutinated - %
Linings/sample (0–2)	Linings/sample (0–2)
E. scabrum 90 (83–97) %	*E. scabrum* 0–49 tests
H. germanica 7 (1–14) %	*H. germanica* 0–15 tests
A. morphogroup *tepida* 2 (0–3) %	
Pollen concentration 58,738 (47,778–77,889) grains/g	Pollen concentration 70,210 (34,267–103,413) grains/g
Heathland – Grassland 14 (10–16) %	Heathland – Grassland 12 (8–17) %
Riparian forest 31 (26–35) %	Riparian forest 37 (32–45) %
Anthropogenic taxa 33 (25–40) %	Anthropogenic taxa 30 (22–37) %
Xuvia	
Xuv-1 (50-25 cm)	Xuv-2 (25-0 cm) (18-1 cm < 100 tests/sample)
Mud 78 (59–90) %	Mud 93 (89–96) %
Sand 18 (11–26) %	Sand 7 (5–11) %
Gravel 4 (0–21) %	Gravel 0%
No. Tests/15 g 190 (19–663)	No. Tests/15 g 28 (2–114)
Marine 82 (32–99) %	Marine 56 (49–67) %
Hyaline 16 (0–72) %	Hyaline 39 (23–50) %
Agglutinated 84 (28–100) %	Agglutinated 61 (50–77) %
Linings/sample 3 (0–10)	Linings/sample (0–1)
E. scabrum 82 (27–99) %	*E. scabrum* 56 (49–67) %
H. germanica 13 (0–54) %	*H. germanica* 38 (22–49) %
A. morphogroup *tepida* 2 (0–10) %	*T. inflata* 3 (1–7) %
S. moniliformis 1 (0–8) %	*A.* morphogroup *tepida* 1 (0.6–2) %
Pollen concentration 33,386 (11,806–67,720) grains/g	Pollen concentration 46,019 (23,580–123,077) grains/g
Heathland – Grassland 18 (11–23) %	Heathland – Grassland 12 (7–17) %
Riparian forest 29 (18–50) %	Riparian forest 42 (37–47) %
Anthropogenic taxa 32 (18–45) %	Anthropogenic taxa 28 (18–37) %

at the base of the Fene core dominate the palynological assemblages (Fig. 5), showing low pine frequencies (anthropogenic taxa), correlating with Holocene pollen records from the Ría of Ferrol and nearby sedimentary environments, such as the Lagoon of Doniños and Ponzos deposit (Gómez-Orellana et al., 2021; Muñoz Sobrino et al., 2022; Santos et al., 2001).

The top core interval Fen-2 (15-0 cm) is also rather muddy (78%). However, it is characterized by the dominance of *E. scabrum* (39%), with decreasing abundances toward the top, *H. germanica* (32%), and *A.* morphogroup *tepida* (27%) (Fig. 5). Hyaline forms compose an average of 61%, with a maximum of 92% at 2 cm deep, and the number of linings is similar compared to the previous unit, with an average of 11/sample. Foraminiferal densities are higher (347–1718 tests/15 g) than those recorded in Fen-1 (Table 4). Taphonomic loss of calcareous taxa occurs in the uppermost 10 cm in most depositional settings (Walker and Goldstein, 1999). Since Fen-2 resembles to surface samples from the IRZ-1 sector (Fig. 3) and the number of linings does not vary significantly regarding the basal zone, it is reasonable to assume that dissolution has not substantially hindered the original foraminiferal assemblages compared to the previous unit. This interval would indicate a similar depositional environment to Fen-1 but under more confined conditions (Diz and Francés, 2008), strongly contrasting with the marine conditions recorded in the surface samples and Holocene cores from the outer sectors of this ría (Mosquera Santé, 2000; Planelles de Miguel, 1996), and the Rías of Arosa, Vigo, and Muros (Diz and Francés, 2008; Lebreiro et al., 2006; Mateu, 1987; Van Voorthuysen, 1973). Heathlands and grasslands show a decreasing trend toward the top core, whereas anthropogenic taxa present higher values (Fig. 5; Table 3). The TOC and TN show concentrations similar to those determined in the previous unit, with a maximum TIC content of 0.24%. However, the $\delta^{13}C$ values slightly decrease to more negative values. Al-normalized concentrations of Zn, Pb and Cu exhibit an increasing upward trend, with values in the top core 10 cm up to four times higher than those found in Fen-1 (Fig. 5). Magnetic susceptibility shows similarly low values in the first part of Fen-2, but it slightly increases from 10 cm deep upward, with a further increase in the uppermost sample, showing a moderate value of $1.43{\cdot}10^{-7}$ m^3 kg^{-1}. This magnetic behavior indicates an increase in the arrival of ferromagnetic phases of likely industrial origin in recent times, coinciding with the highest contents of Zn, Pb, and Cu. Conversely, no substantial changes are observed for Ni along the core, highlighting the absence of significant anthropogenic inputs of this trace metal.

Radiometric data provide a time framework for this core: $^{210}Pb_{xs}$ activity is constant in the uppermost ~15 cm, decreases below this level, and gets canceled at 24-cm depth. The estimated $^{210}Pb_{xs}$ flux is 167 Bq m^{-2} yr^{-1}. Applying the Constant Rate of Supply model (CRS, Appleby and Oldfield, 1978), the chronology of the uppermost 24 cm can be framed in the last ~140 years. Hence, the upper part of Fen-1 (from 24 to 15-cm depth) can be dated between ~1880 ± 27 and 1967 ± 4 CE, whereas Fen-2 should correspond to the time interval after 1967 ± 4 CE until present. The sediment accumulation rate (SAR) increases upward, ranging from 0.02 to 0.13 ± 0.02 cm yr^{-1} in the upper part of Fen-1, to an average of 0.47 ± 0.06 cm yr^{-1} (max. 0.55 cm yr^{-1}) in Fen-2. Unfortunately, the ^{137}Cs shows very low and constant activity values; therefore, it cannot be used as an additional chronostratigraphic marker to corroborate the proposed ages. Considering the previous paleoenvironmental information, the transition from Fen-1 to Fen-2 indicates the evolution of this intertidal area toward more confined and brackish conditions since 1967 ± 4 CE, coinciding with the construction of the As Pías Bridge in 1968. Before 1968 CE, this environment presented an approximately 1-km-wide mouth that connected the outer and middle areas with the inner ría. However, the As Pías Bridge (Fig. 6), a solid structure with a short opening of 300 m, could have functioned as a physical barrier limiting the entrance of marine inflow and favoring the arrival of terrestrial materials with higher sedimentation rates and trace metals retention. The increased inputs of Zn, Pb, and Cu could be derived from the Fene shipyard (Fig. 1), which underwent an essential increase and modernization of its production in the 1960s. Moreover, this information is consistent with the changes observed in the carbon stable isotope ratios, indicating a higher contribution of organic matter from the continental provenance (Lamb et al., 2006; Mackie et al., 2005). Under this scenario, the autochthonous species *A.* morphogroup *tepida* and *H. germanica* might have reacted rapidly increasing their abundances, since their living populations might respond within a small period to rapid changes in the oceanic influence (Cearreta et al., 2002a; Debenay et al., 2006). Likewise, similar compositional changes in the benthic foraminiferal assemblages have been observed in coastal

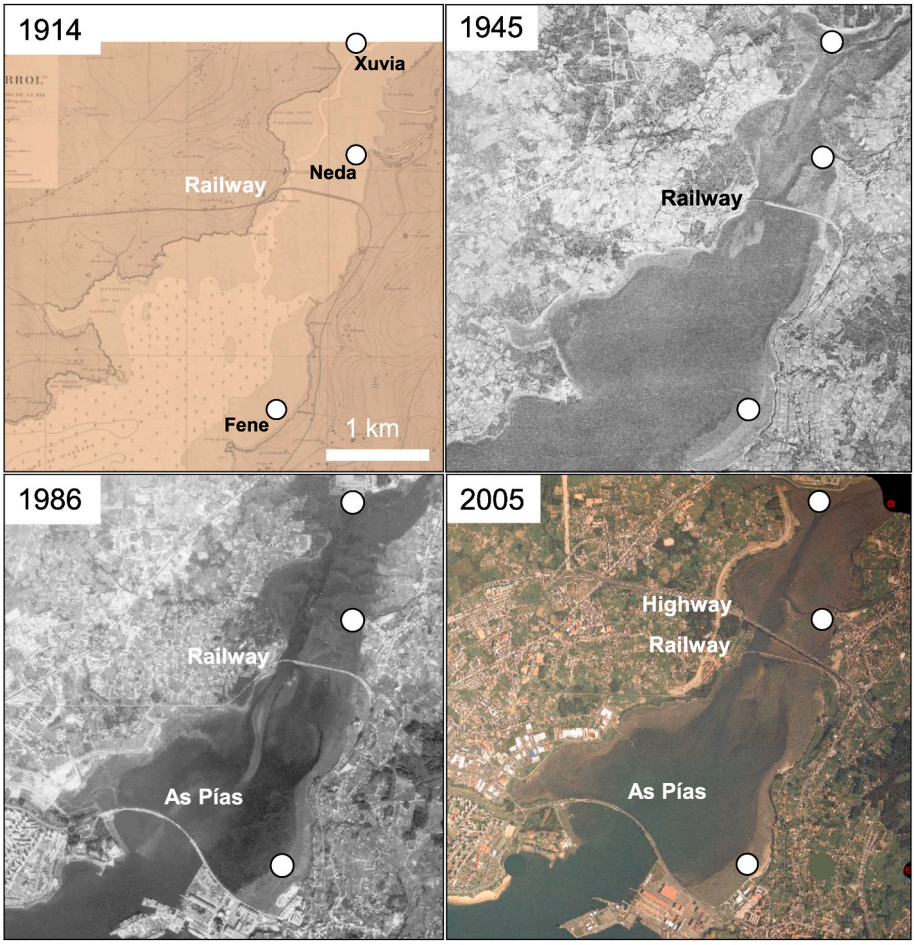

Fig. 6. Historical map (1914: upper left side) and aerial photographs (1945: upper right side, 1986: lower left side, 2005: lower right side) showing the morphological evolution of the inner Ría of Ferrol. The Railway (1913), As Pías (1968) and Highway (2003) bridges are also shown. The location of the three cores (Fene, Neda and Xuvia) is represented by white dots.

Holocene records from the SW Iberian Peninsula, such as in the Albufeira Lagoon, the Mira estuary, the Melides Lagoon, and the Gulf of Cádiz, due to natural barrier developments that limited the seawater exchange (Alday et al., 2006, 2013; Cearreta et al., 2007; Dabrio et al., 2000).

Moreover, the first appearance of high anthropogenic pollen indicator values, primarily represented by *Pinus* and *Eucalyptus*, at 19 cm deep (Fig. 5), temporally corresponds to ~1946 CE. In the 1940s, a process of *Pinus* reforestation initially, and then *Eucalyptus* trees intended for paper pulp and cellulose production, occurred in the region in areas formerly covered by heathland (Rico Boquete, 1995). Consequently, the taxa percentages related to heathlands and grasslands show a marked downward trend, contrasting with the increase recorded for taxa linked to anthropogenic activity (Fig. 5) related to land-use enlargement for agroforestry activities.

4.3. Neda core

This core contains two stratigraphic units or depth intervals: Ned-1 and Ned-2 (Fig. 7). The lowermost Ned-1 (50-46 cm) comprises muddy sediments with a relatively important sand percentage (20.1%) and low gravel content (2.7%) at the base. The foraminiferal densities are very low (44 test/15 g), and only two samples presented more than 100 tests characterized by the dominance of agglutinated wall type foraminifera (>92%) and allochthonous taxa (~90%), primarily *E. scabrum*. Moreover, only one sample contains foraminiferal linings (2), and the TOC values range from 3.2% to 4.6%, whereas the TIC is near zero. Nitrogen contents and $\delta^{13}C$ were 0.28%–0.41% and from −23.3% to −22.6%, respectively. A low concentration and the dominance of riparian forests and anthropogenic taxa groups mark the pollen content. The lowest concentrations of Zn, Pb, and Cu are noticeably higher than those determined in the downcore sediments from Fene (Fen-1), whereas the Ni levels are similar (Table 3). The vertical profiles displayed by Al-normalized contents reflect an increasing trend for Zn and Cu (Fig. 7), whereas Pb presented a differential behavior that might be attributed to the different anthropogenic local sources related to industry or other activities. In turn, magnetic susceptibility values in this basal part of the core are low and remain within the range of those found in Fen-1, indicating a similarly small ferromagnetic content.

Ned-2 (46-0 cm) is a muddy interval exhibiting a negligible presence of benthic foraminifera, with extremely low foraminiferal densities (0–14 tests/15 g) and less than 50 tests/sample (Fig. 7; Table 4). The species present are *E. scabrum* (max. 50 tests) and *H. germanica* (max. 15 tests), and only two samples exhibit foraminiferal linings (1–2). The appearance of common degradation signatures in *E. scabrum* tests is remarkable, exhibiting significant chamber structural damages, such as wall fracturing, collapse and disaggregation (Fig. 4 g, h). One of the primary factors controlling the preservation of agglutinated tests in intertidal and nearshore environments is microbial degradation of organic cement during early diagenesis, leading to physical breakage (Berkeley et al., 2007; Goldstein and Watkins, 1999; Murray and Alve 1999a; Perry et al., 2008). Diz and Francés (2009) associated the disaggregation of *E. scabrum* tests in the nearby Ría of Vigo to microbial activity degradation of their organic membrane. Therefore, the near

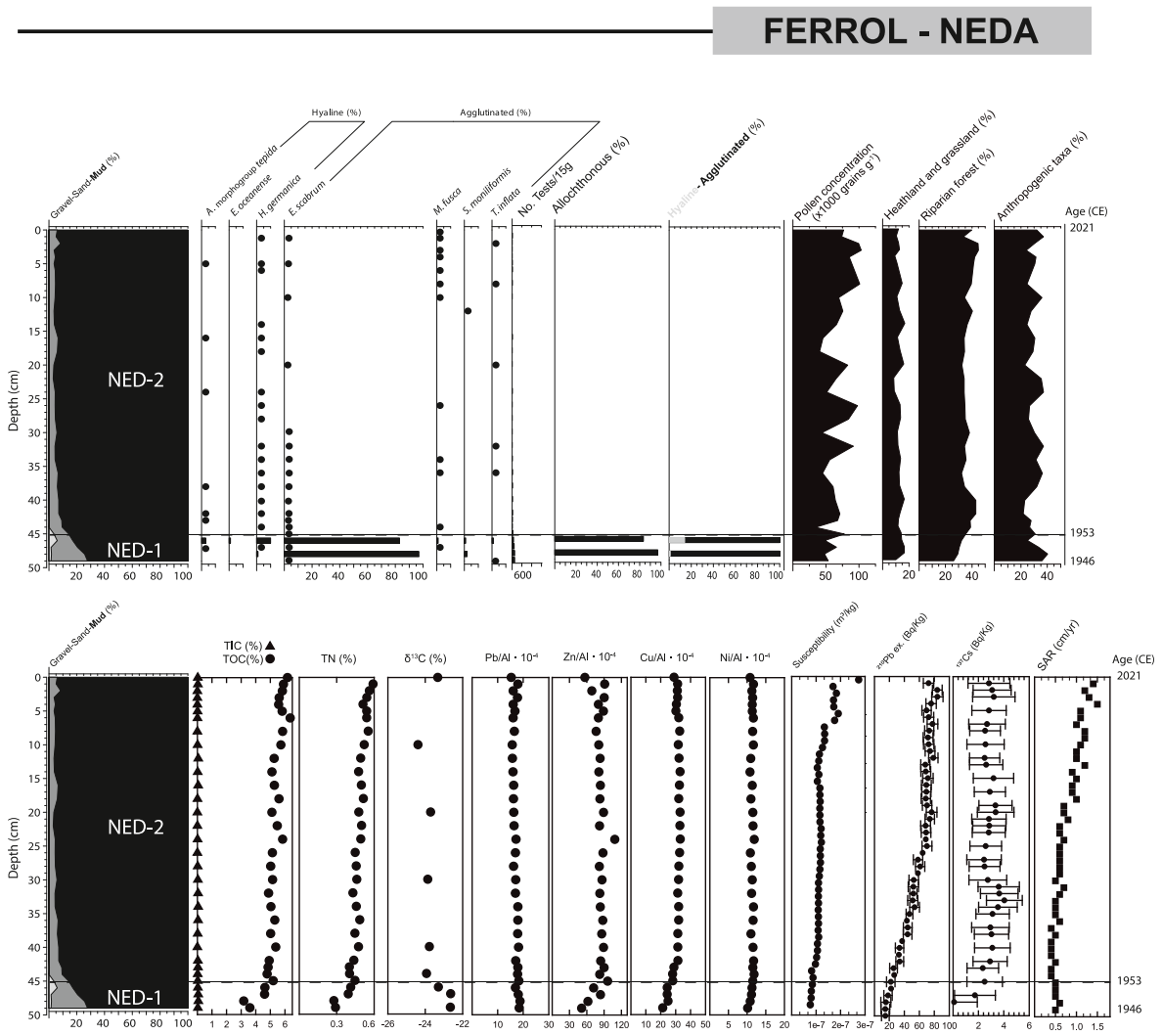

Fig. 7. Vertical distribution of grain-size contents (%), relative abundance of main foraminiferal species (%), pollen concentration (x1000 grain g^{-1} sediment), relative abundance of main Pollen Functional Types (%), TOC, TIC, TN and $\delta^{13}C$ (‰), trace metals, magnetic susceptibility (m^3 kg^{-1}), $^{210}Pb_{xs}$ and ^{137}Cs activities (Bq kg^{-1}) and Sediment Accumulation Rate (cm yr^{-1}) in the Neda core, inner Ría of Ferrol. Black dots represent samples with <100 tests.

absence of agglutinated taxa and the observed taphonomic signatures in Ned-2 could be related to effective microbial activity coinciding with very high TOC (4.8–6.2%) and TN (0.40–0.62%) values, and a shift toward more negative $\delta^{13}C$ ratios (−24.4 to −23.3‰). Also, the near total absence of calcareous taxa in this zone is noticeable. Since they exhibit high abundances in surface samples from IRZ-2, these data confirm the existence of underlying burial processes driving their preservation favored by low TIC. Several studies have confirmed the extensive bacterial activity occurring in the Galician rías capable of altering local microenvironment conditions (e.g., Álvarez-Iglesias and Rubio, 2012; Mohamed et al., 2011; Otero et al., 2009; Varela et al., 2003). The dissolution of calcareous taxa in this zone could be related to carbonate-undersaturated porewater conditions and corrosive/low pH microenvironments caused by organic matter metabolization by bacteria, leading to lower biogenic carbonates (Diz and Francés, 2009; Reaves, 1986; Sanders, 2003), as inferred in the Ría of Vigo (Álvarez-Iglesias et al., 2006). These burial conditions might cause a shift in the foraminiferal test balance preservation toward the destruction of tests when compared with sediments characterized by a high biogenic production of these organisms (Loubere and Gary, 1990), as observed in local surface samples.

The upper part of the Neda core (Ned-2) exhibits slightly higher concentrations of pollen than Ned-1, which could be related to a greater extent of riparian forest taxa due to the continental influence in this innermost area (Penaud et al., 2020). Al-normalized concentrations of trace metals exhibit near homogeneous vertical profiles (Fig. 7). Magnetic susceptibility values are also slightly higher in Ned-2 than in previous Ned-1, from 43 cm deep upward, and they show additional increases from 10 cm deep upward, reaching its maximum value in the topmost sample.

The distribution of $^{210}Pb_{xs}$ activity is constant in the upper ~20 cm, with decreasing values from this depth downward but not canceling its activity at the core base. The overall $^{210}Pb_{xs}$ flux is 577 Bq m^{-2} yr^{-1}, much higher than the amount calculated for the Fene core (167 Bq m^{-2} yr^{-1}). The probable absolute ages have been obtained by estimating the total inventory: Ned-1 can be framed between the early 1940s and 1953 CE, whereas the Ned-2 interval can be dated between 1953 and 2021 CE. The SAR values increase from 0.6 cm yr^{-1} in Ned-1 to 1.5 cm yr^{-1} in Ned-2. This increasing trend in the SAR and the maximum values from Neda (1.5 cm yr^{-1}), more than two times higher than the average proposed for this inner part (0.62 cm yr^{-1}; Álvarez-Vázquez et al., 2020), indicates a vital accumulation of sediment in this area during recent times. The increased depositional rates might have reduced and masked the fingerprint of anthropogenic inputs, causing an apparent homogeneity in the trace metal contents (Fig. 7). In this sense, very high fluxes of $^{210}Pb_{xs}$ (~660–1100 Bq m^{-2} yr^{-1}) and increasing SAR were detected in

sediment cores from the nearby Rías of Ares, Betanzos, and Cedeira, which were attributed to historical land-use changes in their respective catchment basins (Álvarez-Vázquez et al., 2017).

4.4. Xuvia core

This core can also be divided into two stratigraphic units or depth intervals: Xuv-1 and Xuv-2 (Fig. 8). The lower unit, Xuv-1 (50-25 cm) shows high sand (av. 18.4%) and gravel (av. 3.4%, max. 20.8%) contents and is characterized by *E. scabrum* (81.8%) and *H. germanica* (15.1%) as dominant species, with the accessory taxa *A.* morphogroup *tepida* (2.8%) and *S. moniliformis* (1.4%). Allochthonous marine forms range from 32% to >99%, presenting low to moderate foraminiferal densities (19–663 test/15 g) and many linings (max. 10/sample). The TOC and TN values range from 1.83% to 5.16% and 0.12%–0.44%, respectively, whereas TIC is near zero and $\delta^{13}C$ considerably decreases toward the top of the unit. According to these data, the depositional environment was a muddy-fine-sandy intertidal flat with high marine influence (Diz and Francés, 2008). The palynological content exhibits high abundances (approximately 30%) of anthropogenic taxa (Table 4), indicating a significant human influence in the catchment basin.

Al-normalized concentrations of Pb, Zn, and Cu increase upward, reaching maximum values, distinctly higher than those recorded in the surface samples and the other two cores at approximately 25 cm deep (Fig. 8). Magnetic susceptibility and, hence, ferromagnetic content show very low values (below $1{\cdot}10^{-7}$ m^3 kg^{-1}, similar to those observed in the Fen-1 and Ned-1 intervals) between 50 and 46 cm deep, followed by a first increase to moderate values of $1.41–2.59{\cdot}10^{-7}$ m^3 kg^{-1} between 46 and 40 cm deep. Much more dramatic, although fluctuating, increases are observed from 40 to 25 cm, with three maximum peaks at 37–36, 31–30 and 25-24 cm deep. Microplastics contents range from 0 to 104 particles kg^{-1} d.w. sediment, with the first appearance of microplastics at 33 cm deep and a slight increase toward the topmost section of Xuv-1.

However, Xuv-2 (25-0 cm) is a dominantly muddy interval, characterized by a mixture of *E. scabrum* (56%) and *H. germanica* (38%) as the primary taxa, with lower marine species abundance (56%). Low-salinity forms (e.g., *T. inflata*, *S. moniliformis,* and *Haplophragmoides wilberti*) reach a maximum of 9.6%, indicating a higher continental influence than in the basal zone (Debenay et al., 2006). The decreasing abundances of *E. scabrum* and marine taxa and the dominance of mud grain-size sediments in this unit indicate a more restricted and brackish depositional environment (Diz and Francés, 2008). Likewise, the elevated abundances of riparian forest pollen confirm the higher influence of the continental end-member. From 18 cm deep upward, the foraminiferal density (4–28 test/15 g) is very low, accompanied by the almost total absence of linings and higher TOC and TN values,

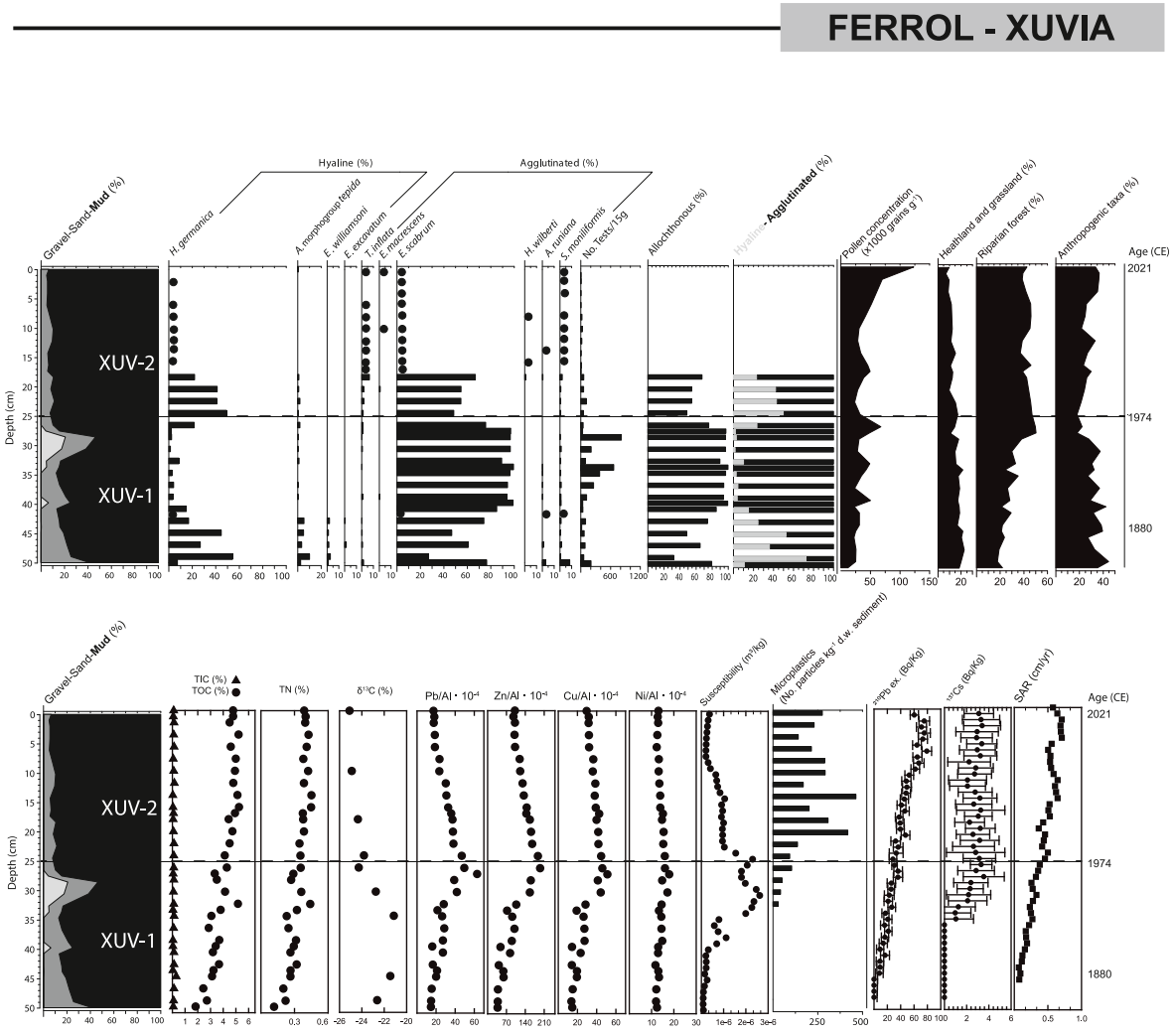

Fig. 8. Vertical distribution of grain-size contents (%), relative abundance of main foraminiferal species (%), pollen concentration (x1000 grain g^{-1} sediment), relative abundance of main Pollen Functional Types (%), TOC, TIC, TN and $\delta^{13}C$ (%), trace metals, magnetic susceptibility (m^3 kg^{-1}), microplastics content (particles kg^{-1} d.w. sediment), $^{210}Pb_{xs}$ and ^{137}Cs activities (Bq kg^{-1}) and Sediment Accumulation Rate (cm yr^{-1}) in the Xuvia core, inner Ría of Ferrol. Black dots represent samples with <100 tests.

resembling the Ned-2 unit from the Neda core. $\delta^{13}C$ exhibits very low and constant values, similar to the Ned-2. In this uppermost section, the primary species from the previous interval are present: *E. scabrum* (max. 43 tests) and *H. germanica* (max. 18 tests). The scarce number of calcareous and agglutinated taxa, and the taphonomic signatures of physical breakage (Fig. 4 g, h; wall fracturing, collapse, and disaggregation) due to the loss of the organic cement observed in *E. scabrum* (Fig. 3), coincide with the higher TOC and TN values. This nearly azoic unit indicates a shift toward the foraminiferal test destruction during burial and could result from carbonate-undersaturated porewater conditions and enhanced microbial activity, as inferred for Ned-2.

The vertical profiles displayed by Al-normalized Pb, Zn, and Cu along Xuv-2 are similar in shape, with diminishing concentrations toward the uppermost part of the sequence (Fig. 8). Magnetic susceptibility, after reaching a relative maximum at 25-24 cm, shows a first step of strong decrease in the lowest centimeters of Xuv-2, with values of 6.48–10.52·10^{-7} m^3 kg^{-1} between 23 and 10 cm deep. Afterward, the values decrease further in a second step, reaching 2.06·10^{-7} m^3 kg^{-1} at 8-7 cm deep. From this depth upward, the uppermost part of the Xuv-2 interval is marked by a steady but minor increase in susceptibility, reaching up to 3.68·10^{-7} m^3 kg^{-1} at the surface centimeter (Fig. 8). The density of microplastics considerably increases from 25 cm deep upward (Fig. 8; Table 3), from 94 to 463 particles kg^{-1} d.w. sediment. The highest frequencies, corresponding to fibers (81% frequency of occurrence, maximum length of 5 mm), match the importance of microfibers in marine environments described by Gago et al. (2018). A tangle of fibers (aggregate of fibers with irregular sizes) with fewer of fragments (12%) and films (7%) is also present, as illustrated in Fig. S1 of the Supplementary Material.

The $^{210}Pb_{xs}$ activity is constant in the uppermost 9 cm, decreasing at 9 cm deep and canceling its activity at 44 cm deep. The overall $^{210}Pb_{xs}$ flux is 290 Bq m^{-2} yr^{-1}. The chronology of this core can be framed between 1880 ± 23 and 2021 CE by applying the CRS model, and the limit between Xuv-1 and Xuv-2 corresponds to 1974 ± 3 CE. The SAR exhibits an increasing trend upward, ranging from 0.05 ± 0.01 to 0.43 ± 0.07 cm yr^{-1} in Xuv-1, with higher values at the topmost section (average: 0.68 ± 0.06 cm yr^{-1}) of Xuv-2, indicating a progressive sediment infill. The ^{137}Cs appears at 33 cm deep (1946 ± 6 CE) and shows very low and constant activity values upward; therefore, its use as a chronostratigraphic marker is problematic. This artificial radionuclide could have migrated downward (Hancock et al., 2011) because the first appearance of ^{137}Cs in a sediment core is thought to occur globally at ~1955 CE (Foucher et al., 2021).

According to our chronological model, the increasing trend in trace metals and susceptibility (Fig. 8), with their maximum values occurring between 1951 ± 5 and 1975 ± 3 CE, could be related to the historical industrial development of Ferrol and nearby localities around the ría. This trend could also be marked by direct industrial waste discharges of slags into the inner ría, as reported by Graña and Macías (1987a), close to the steel factory Megasa Siderúrgica Narón Xuvia (Fig. 1), locally altering the hydrochemical conditions. The industrial growth of Ferrol was primarily linked to the development of steel-metallurgical factories and shipyards (Cardesín, 2004). Most industries are in the middle and inner ría areas, and their activities involve several inorganic contaminants (e.g., Pb, Zn, and Cu) during manufacturing processes, which could easily be released into the environment. Likewise, the presence and increasing abundance of microplastics highlight to a period of intensification of plastic usage and production, which globally started in the 1950s (Zalasiewicz et al., 2016). Finally, the decreasing trend in trace metals and magnetic susceptibility observed since the late 1970s and 1980s in Xuvia could be related to the regional industrial decline (Cardesín, 2004). These trends match the trace metal fluxes proposed by Álvarez-Vázquez et al. (2017, 2020) for the 20th century in the Ferrol and nearby rías.

4.5. Environmental quality and management of the inner Ría of Ferrol

The multidisciplinary study of surface samples and vertical cores allows for achieving a combined geographic and stratigraphic perspective of environmental and ecological condition changes of coastal areas through space and time, offering an excellent framework for future management policies and strategies. Regarding the environmental quality of the inner Ría of Ferrol, the number of living foraminifera (standing crop) ranges from moderate to very high values, presenting higher numbers in IRZ-1 than in IRZ-2, indicating the marine water influence, as shown by the total number of transported marine dead tests. Generally, the foraminiferal standing crops found here are similar or even higher than those in undisturbed, low-anthropized or nearly regenerated estuaries from the northern Iberian coast (Cearreta, 1988; Cearreta et al., 2021; Irabien et al., 2018; Leorri et al., 2008) and elsewhere in the northern Atlantic realm (Debenay et al., 2006; Leorri et al., 2010; Murray and Alve, 2000). This result indicates scarce anthropogenic influences affecting the overall current environmental quality conditions. However, sediments collected in sampling station 8 exhibit extremely low numbers of foraminifera (34 living individuals/80 cm^3 and 18 dead tests/80 cm^3) and a high content of organic carbon, probably associated with the nearby influence of the wastewater treatment plant at Neda (Fig. 1). Therefore, further studies are recommended in this area to gain insights into the potential role of this facility in the biogeochemical functioning of the inner ría.

The recent sedimentary evolution of the inner Ría of Ferrol shows a noticeable increasing continental influence from 1968 CE onward in its lower sector due to the construction of the As Pías Bridge. Physical barriers, such as bridges and dams cause various environmental perturbations involving reduced salinity, water quality variations, differences in habitat structure, biotic composition, and higher sedimentation rates. Pérez Alberti et al. (2002) warned about the potential sediment infilling of the inner Ría of Ferrol due to the construction of different bridges (Fig. 1: As Pías, Railway, and Highway bridges) and several land fillings that could limit the sediment transport from the innermost toward the middle and outer sectors of this ría. According to our results, the reduced marine influx in Fene, the increased sedimentary accumulation recorded in Neda and Xuvia, and the consequent higher sedimentation rates could all have resulted from the progressive sediment infilling of this artificially semiconfined area, where dredging activities could be necessary in the near future to maintain the estuarine conditions. Therefore, this area accumulates fine-grained sediments leading to extensive mudflats, probably enhanced due to the physical barriers limiting the sediment transport toward the ocean. Although further research is needed, the rise in sediment accumulation rates in the inner ría during the last decades is according to the regional tendency observed in the Galician coast derived from an anthropogenic influence (Álvarez-Iglesias et al., 2007, 2020; Álvarez-Vázquez et al., 2017). The increasing trends could be conditioned by land-use changes in the hydrographic basins, as suggested by vegetation shifts in response to regional land-use changes related to the reforestation plans started in the 1940s.

The increasing organic carbon and TN concentration observed in the innermost areas of the Ría of Ferrol since the beginning of the 20th century could be related to the crucial demographic growth experienced by the localities surrounding this ría because of the industrial development and the total absence of water sewage treatment until the early 21st century (Pérez Alberti et al., 2002). The recorded organic carbon values correlate with those estimated previously by Graña and Macías (1987b), who determined a remarkable accumulation of organic carbon in the inner and more confined intertidal environments of Ferrol due to untreated urban and industrial waste discharges. This same effect was also observed worldwide in coastal areas subjected to the influence of uncontrolled urban expansion receiving untreated effluents (Bartolomé et al., 2006; Brush, 2009; Pérez et al., 2022). These increases in organic matter are accompanied by a $\delta^{13}C$ resemblant to continental and sewage

sources (Graham et al., 2001). Untreated sewage was a serious matter of concern in Galician rías, causing a high organic matter content, high numbers of heterotrophic bacteria, fecal coliforms, and streptococci in their sediments and waters, clear indicators of fecal pollution (e.g., Combarro et al., 1993). In the Ría of Ferrol, Graña and Macías (1987a) reported very low levels of dissolved oxygen near the anthropogenic waste effluents, whereas degraded conditions were invoked to continue at least until the late 2010s due to a lack of wastewater treatment plants, even breaching the European Community law (Greenpeace, 2005a; 2005b; Ecologistas en Acción, 2016). The presence of intervals with scarce foraminifera in sediments from different human-impacted coastal areas has been attributed to a detrimental environmental state and pollution (e.g., Alve, 1995; Mojtahid et al., 2008; Ruiz et al., 2008; Serrano, 2020). Cearreta et al. (2002b) concluded that oxygen limitation was the primary cause of long-term defaunation in the heavily-polluted Bilbao estuary (northern Spain). However, in the inner Ría of Ferrol, foraminifera do not seem to have directly experienced a severe impact by untreated urban and industrial effluents. Since the autochthonous species (e.g., *H. germanica* and *A.* morphogroup *tepida*) and transported dead tests (e.g., *E. scabrum*) are absent, their near disappearance in the innermost areas seems to be related to very active taphonomic processes. The nearly azoic intervals could have been induced through microbial activity and porewater geochemistry conditions during burial, favored by high organic matter concentrations from sewages. These taphonomic activities are highly rapid and effective, even affecting the topmost centimetres of the sediments. Although adverse environmental conditions during the last decades in the innermost area cannot be discarded, further multidisciplinary research could shed light on the ecological and taphonomic impact of organic matter from untreated effluents on benthic foraminifera.

Regarding the geochemical quality of the sediments and considering that differences in the analytical procedures used might complicate a direct comparison, the Cu, Pb, and Zn concentrations in the lower half of the Fene core (Fen-1) are comparable to those proposed as local background values and others from scarcely-polluted nearby rías presented by different authors (Table 3). These geochemical values in Fene are accompanied by a pollen assemblage similar to the Holocene records. Notwithstanding that the rest of the analyzed samples (surface and core sediments) exhibit enhanced Cu, Pb, and Zn levels, the highest concentrations of these trace metals are far below those determined in other industrialized estuaries and rías of Galicia, the Cantabrian coast (Table 3), and in other Atlantic coastal areas (Davis et al., 2000). The only exception to this general trend is at 10–30 cm deep in the Xuvia core ($n = 12$), where sediments exhibit Zn contents exceeding the Effects Range Median (ERM) threshold established by Long et al. (1995) (Table 3), above which adverse effects on biota frequently occur. According to the classification of dredged materials in the Spanish framework (Buceta et al., 2015), concentrations like these, between action levels B and C (Table 3), represent an uncertainty range about its possible effects on marine biota, for which resolution bioassays should be conducted. Furthermore, the abundance of microplastics in Xuvia (mean 138 ± 28 particles kg^{-1} d.w. sediment; Table 3) is higher than the densities measured in the coastal and marine areas from southern Galicia (70 ± 74 kg^{-1} particles d.w. sediment; Carretero et al., 2021) and the Bay of Biscay (average 67 ± 76 particles kg^{-1} d.w. sediment; Phuong et al., 2018), evidencing the significant accumulation of these emerging contaminants in the Ría of Ferrol.

Dredging activities could provoke the resuspension of stored pollutants into the water column, leading to their bioavailability for biotic communities (Nayar et al., 2003), with consequent risks for organisms and human health by entering the food chain. Since microplastics interact with trace metals, functioning as vectors by adsorption (Brennecke et al., 2016), their coincident abundant presence with Zn concentrations exceeding the ERM highlights the importance of environmental monitoring studies. The environmental risk assessment of these processes in the Galician rías, where a vital proportion of their economy depends on the coastal ecosystem services, particularly relying on marine aquaculture and fishing (Surís-Regueiro and Santiago, 2014), is crucial and pending. Regardless of the results to be obtained, the appearance of a hidden amount of more contaminated sediments in the innermost sector illustrates the need for considering spatial trends and stratigraphic historical variations and their ecotoxicological implications when addressing the environmental management of the coastal domain.

5. Conclusions

Recent coastal sediments from the industrialized inner Ría of Ferrol provide an excellent natural archive to explore multiple human-driven imprints, since they are exposed to a restricted water exchange with the nearby shelf. The multiproxy analysis of modern intertidal surface samples and cores allowed the following:

- Assess the current environmental quality of the sediments, revealing a dominant natural ría-estuarine dynamics controlling the benthic foraminiferal distribution and abundance, with overall standing crops typical from barely undisturbed or nearly regenerated estuaries. The surface sediments exhibit moderate trace metal concentrations but high ferromagnetic material concentrations in the innermost area due to industrial activities developed in the surroundings.
- Accomplish a historical comprehensive perspective of the primary anthropogenic impacts at local and regional scales. The sedimentary sequences recorded at a local level: i) physical interventions in constructing the As Pías Bridge (1968) and ii) the industrial-urban growth of Ferrol City and other localities surrounding the ría with notable geochemical and magnetic imprints. Vegetation shifts were detected at a regional scale by introducing anthropogenic taxa for industrial purposes at the expense of former heathlands associated with land-use changes. These processes could have caused the increased sedimentation rates, matching the general trend observed in the northwestern Iberian margin.
- Determine some pollutants in the innermost area, with Zn and microplastics as the primary environmental concern, which could be easily released by potential dredging activities leading to their possible bioavailability.
- Recognize nearly azoic stratigraphic intervals likely caused by strong taphonomic biases, leading to foraminiferal test destruction. Although historical adverse environmental conditions cannot be discarded, this study reinforces involving a taphonomic approach when dealing with paleoenvironmental reconstructions in polluted areas to discriminate natural *post-mortem* processes (e.g., calcareous dissolution and/or disaggregation of agglutinated tests) from anthropogenic impacts on benthic communities (e.g., derived from pollution and/or oxygen depletion).

Declaration of competing interest

The authors declare that they have no known competing financial interests or personal relationships that could have appeared to influence the work reported in this paper.

Acknowledgements

This research was financially supported by RTI2018-095678-B-C21, MCIU/AEI/FEDER, UE (MINECO) and IT1616-22 (EJ/GV) projects. Jon Gardoki and Carlos Galaz are supported by predoctoral fellowships granted by the Basque Government (PRE_2020_1_0035) and Mexican Consejo Nacional de Ciencia y Tecnología (CONAHCYT 771105), respectively. Jordina Belmonte is also thanked for sharing laboratory facilities for pollen extraction at the Autonomous University of Barcelona. Filipa Bessa was supported by the University of Coimbra through

the contract IT057-18-7252 and Portuguese Foundation for Science and Technology (FCT), I.P. through the strategic projects UIDB/04292/2020 and UIDP/04292/2020 granted to MARE and LA/P/0069/2020, granted to the Associate Laboratory ARNET. María Celia Besteiro (University of Santiago de Compostela, Spain) is thanked for the historical micropaleontological information kindly supplied. It is contribution 57 of the Geo-Q Zentroa Research Unit (Joaquín Gómez de Llarena Laboratory). The manuscript was revised by the Language Editing Services of Elsevier. We are grateful to the Associate Editor (Ángel Borja) and two anonymous reviewers for their constructive comments and suggestions that contributed to improve the original manuscript.

Appendix A. Supplementary data

Supplementary data related to this article can be found at https://doi.org/10.1016/j.csr.2023.105098.

Table A1
Reference list of identified estuarine (autochthonous) and marine (allochthonous) foraminiferal species in the inner Ría of Ferrol (Galicia, Spain) grouped by wall type.

ESTUARINE (Autochthonous)
Agglutinated test
Entzia macrescens (Brady) = *Trochammina inflata* (Montagu) var. *macrescens* Brady, 1870
Haplophragmoides canariensis (d'Orbigny) = *Nonionina canariensis* d'Orbigny, 1839
Haplophragmoides wilberti Andersen, 1953
Lepidodeuterammina ochracea (Williamson) = *Rotalina ochracea* Williamson, 1858
Miliammina fusca (Brady) = *Quinqueloculina fusca* Brady, 1870
Scherochorella moniliformis (Siddall) = *Reophax moniliforme* Siddall, 1886
Tiphotrocha comprimata (Cushman & Brönnimann) = *Trochammina comprimata* Cushman and Brönnimann, 1948
Trochammina inflata (Montagu) = *Nautilus inflatus* Montagu, 1808
Porcellaneous test
Quinqueloculina seminulum (Linnaeus) = *Serpula seminulum* Linnaeus, 1758
Hyaline test
Ammonia morphogroup *tepida* (Cushman) = *Rotalia beccarii* var. *tepida* Cushman, 1926
Bolivina britannica Macfadyen, 1942
Bolivina pseudoplicata Heron-Allen and Earland, 1930
Elphidium excavatum (Terquem) = *Polystomella excavata* Terquem, 1875
Elphidium margaritaceum Cushman, 1930
Elphidium oceanense (d'Orbigny in Fornasini) = *Polystomella oceanensis* d'Orbigny, 1826
Elphidium williamsoni Haynes, 1973
Haynesina germanica (Ehrenberg) = *Nonionina germanica* Ehrenberg, 1840
MARINE (Allochthonous)
Agglutinated test
Ammobaculites agglutinans (d'Orbigny) = *Spirolina agglutinans* d'Orbigny, 1846
Ammoscalaria runiana (Heron-Allen & Earland) = *Haplophragmium runianum* Heron-Allen and Earland, 1916
Deuterammina rotaliformis (Heron-Allen & Earland) = *Trochammina rotaliformis* Heron-Allen and Earland, 1911
Eggerelloides scabrum (Williamson) = *Bulimina scabra* Williamson, 1858
Pseudobolivina fusiformis (Chaster) = *Textularia fusiformis* Chaster, 1892
Reophax fusiformis (Williamson) = *Proteonina fusiformis* Williamson, 1858
Textularia sp.
Porcellaneous test
Adelosina bicornis (Walker & Jacob) = *Serpula bicornis* Adams, 1798
Milionella subrotunda (Montagu) = *Vermiculum subrotundum* Montagu, 1803
Quinqueloculina lata Terquem, 1876
Triloculina oblonga (Montagu) = *Vermiculum oblongum* Montagu, 1803
Hyaline test
Asterigerinata mamilla (Williamson) = *Rotalina mamilla* Williamson, 1858
Bolivina difformis (Williamson) = *Textularia variabilis* var. *difformis* Williamson, 1858
Bolivina spathulata (Williamson) = *Textularia variabilis* var. *spathulata* Williamson, 1858
Bolivina variabilis (Williamson) = *Textularia variabilis* Williamson, 1858
Bolivina sp.
Bolivinellina pseudopunctata (Höglund) = *Bolivina pseudopunctata* Höglund, 1947
Bolivinellina translucens (Phleger & Parker) = *Bolivina translucens* Phleger and Parker, 1951
Bulimina gibba Fornasini, 1902
Bulimina marginata d'Orbigny, 1826
Buliminella elegantissima (d'Orbigny) = *Bulimina elegantissima* d'Orbigny, 1839
Cancris auricula (Fichtel & Moll) = *Nautilus auricula* Fichtel & Moll, 1798
Cassidulina obtusa Williamson, 1858
Cibicides refulgens Montfort, 1808
Cibicidoides wuellerstorfi (Schwager) = *Anomalina wuellerstorfi* Schwager, 1866
Cribroelphidium gerthi (van Voorthuysen) = *Elphidium gherti* Van Voorthuysen, 1973
Eilohedra vitrea (Parker) = *Epistominella vitrea* Parker, 1953
Elphidium advenum (Cushman) = *Polystomella advena* Cushman, 1922
Elphidium crispum (Linnaeus) = *Nautilus crispus* Linnaeus, 1758
Elphidium earlandi Cushman, 1936
Elphidium macellum (Fichtel & Moll) = *Nautilus macellum* Fichtel & Moll, 1798
Elphidium translucens Natland, 1938
Elphidium sp. 1

(*continued on next page*)

Table A1 (*continued*)

ESTUARINE (Autochthonous)
Elphidium sp. 2
Favulina melo (d'Orbigny) = *Oolina melo* d'Orbigny, 1839
Fissurina lucida (Williamson) = *Entosolenia marginata* var. *lucida* Williamson, 1848
Fissurina marginata (Montagu) = *Vermiculum marginatum* Montagu, 1803
Fissurina orbignyana Seguenza, 1862
Fissurina sp. 1
Fissurina sp. 2
Gavelinopsis praegeri (Heron-Allen & Earland) = *Discorbina praegeri* Heron-Allen and Earland, 1913
Haynesina depressula (Walker & Jacob) = *Nautilus depressulus* Walker & Jacob, 1798
Hopkinsina atlantica Cushman, 1944
Lobatula lobatula (Walker & Jacob) = *Nautilus lobatulus* Walker & Jacob, 1798
Nonion boueanum (d'Orbigny) = *Nonionina boueana* d'Orbigny, 1846
Nonion sp.
Planorbulina mediterranensis d'Orbigny, 1826
Rosalina anomala Terquem, 1875
Spirillina vivipara Ehrenberg, 1843
Stainforthia fusiformis (Williamson) = *Bulimina pupoides* var. *fusiformis* Williamson, 1858
Trifarina angulosa (Williamson) = *Uvigerina angulosa* Williamson, 1858

References

Alday, M., Cearreta, A., Cachão, M., Freitas, M.C., Andrade, C., Gama, C., 2006. Micropaleontological record of Holocene estuarine and marine stages in the Corgo do Porto rivulet (Mira River, SW Portugal). Estuar. Coast Shelf Sci. 66, 532–543. https://doi.org/10.1016/j.ecss.2005.10.010.

Alday, M., Cearreta, A., Freitas, M.C., Andrade, C., 2013. Modern and late Holocene foraminiferal record of restricted environmental conditions in the Albufeira Lagoon, SW Portugal. Geol. Acta 11 (1), 75–84. https://doi.org/10.1344/105.000001754.

Alejo, I., Austin, W.E.N., Francés, G., Villas, E., 1999. Preliminary investigations of the recent foraminifera of baiona Bay, N.W. Spain. J. Coast Res. 15 (2), 413–427.

Álvarez-Iglesias, P., Rubio, B., Vilas, F., 2003. Pollution in intertidal sediments of San Simón Bay (Inner Ria de Vigo, NW of Spain): total heavy metal concentrations and speciation. Mar. Pollut. Bull. 46, 491–521. https://doi.org/10.1016/S0025-326X(03)00004-3.

Álvarez-Iglesias, P., Rubio, B., Pérez-Arlucea, M., 2006. Reliability of subtidal sediments as "geochemical recorders" of pollution input: san Simón Bay (Ría de Vigo, NW Spain). Estuar. Coast Shelf Sci. 70 (3), 507–521. https://doi.org/10.1016/j.ecss.2006.07.001.

Álvarez-Iglesias, P., Quintana, B., Rubio, B., Pérez-Arlucea, M., 2007. Sedimentation rates and trace metal history in intertidal sediments from San Simon Bay (Ria de Vigo, NW Spain) derived from ^{210}Pb and ^{137}Cs chronology. J. Environ. Radioact. 98, 229–250. https://doi.org/10.1016/j.jenvrad.2007.05.001.

Álvarez-Iglesias, P., Rubio, B., 2012. Early diagenesis of organic-matter-rich sediments in a ría environment: organic matter sources, pyrites morphology and limitation of pyritization at depth. Estuar. Coast Shelf Sci. 100, 113–123. https://doi.org/10.1016/j.ecss.2012.01.005.

Álvarez-Iglesias, P., Andrade, A., Rey, D., Quintana, B., Bernabeu, A.M., López-Pérez, A. E., Rubio, B., 2020. Assessment and timing of the anthropogenic imprint and fisheries richness in marine sediments from Ría de Muros (NW Iberian Peninsula). Quat. Int. 566–567, 337–356. https://doi.org/10.1016/j.quaint.2020.05.005.

Álvarez-Vázquez, M.A., Caetano, M., Álvarez-Iglesias, P., Pedrosa-García, M.C., Calvo, S., de Uña-Álvarez, E., Quintana, E., Vale, C., Prego, R., 2017. Natural and Anthropocene fluxes of trace elements in estuarine sediments of Galician Rias. Estuar. Coast Shelf Sci. 198 (B), 329–342. https://doi.org/10.1016/j.ecss.2016.08.022.

Álvarez-Vázquez, M.A., Álvarez-Iglesias, P., De Uña-Álvarez, E., Quintana, B., Caetano, M., Prego, R., 2020. Industrial supply of trace elements during the "Anthropocene": a record in estuarine sediments from the Ria of Ferrol (NW Iberian Peninsula). Mar. Chem. 223, 103825 https://doi.org/10.1016/j.marchem.2020.103825.

Alve, E., 1991. Benthic foraminifera in sediment cores reflecting heavy metal pollution in Sorfjord, western Norway. J. Foraminifer. Res. 21 (1), 1–19.

Alve, E., 1995. Benthic foraminiferal responses to estuarine pollution; a review. J. Foraminifer. Res. 25 (3), 190–203. https://doi.org/10.2113/gsjfr.25.3.190.

Alve, E., Murray, J.W., 1999. Marginal marine environments of the Skagerrak and Kattegat: a baseline study of living (stained) benthic foraminiferal ecology. Palaeogeogr. Palaeoclimatol. Palaeoecol. 146, 171–193. https://doi.org/10.1016/S0031-0182(98)00131-X.

Andrews, J.E., Samways, G., Dennis, P.F., Maher, B.A., 2000. Origin, abundance and storage of organic carbon and sulphur in the Holocene Humber Estuary: emphasizing human impact on storage changes. Geol. Soc., Lond. Special Publ. 166 (1), 145–170. https://doi.org/10.1144/GSL.SP.2000.166.01.09.

Appleby, P.G., Oldfield, F., 1978. The calculation of lead-210 dates assuming a constant rate of supply of unsupported ^{210}Pb to the sediment. Catena 5 (1), 1–8. https://doi.org/10.1016/S0341-8162(78)80002-2.

Avnaim-Katav, S., Gehrels, W.R., Brown, L.N., Fard, E., MacDonald, G.M., 2017. Distributions of salt-marsh foraminifera along the coast of SW California, USA: implications for sea-level reconstructions. Mar. Micropaleontol. 131, 25–43. https://doi.org/10.1016/j.marmicro.2017.02.001.

Bartolomé, L., Tueros, I., Cortazar, E., Rapodos, J.C., Sanz, J., Zuloaga, O., de Diego, A., Etxebarria, N., Fernández, L.A., Madariaga, J.M., 2006. Distribution of trace organic contaminants and total mercury sediments from the Bilbao and Urdaibai Estuaries (Bay of Biscay). Mar. Pollut. Bull. 52 (9), 1111–1117. https://doi.org/10.1016/j.marpolbul.2006.05.024.

Beiras, R., Fernández, N., Bellas, J., Besada, V., González-Quijano, A., Nunes, T., 2003a. Integrative assessment of marine pollution in Galician estuaries using sediment chemistry, mussel bioaccumulation, and embryo-larval toxicity bioassays. Chemosphere 52 (7), 1209–1224. https://doi.org/10.1016/S0045-6535(03)00364-3.

Beiras, R., Bellas, J., Fernández, N., Lorenzo, J.I., Cobelo-García, A., 2003b. Assessment of coastal marine pollution in Galicia (NW Iberian Peninsula); metal concentrations in seawater, sediments and mussels (*Mytilus galloprovincialis*) versus embryo-larval bioassays using *Paracentrotus lividus* and *Ciona intestinalis*. Mar. Environ. Res. 56, 531–553. https://doi.org/10.1016/S0141-1136(03)00042-4.

Bellas, J., Fernández, N., Lorenzo, I., Beiras, R., 2008. Integrative assessment of coastal pollution in a Ría coastal system (Galicia, NW Spain): correspondence between sediment chemistry and toxicity. Chemosphere 72 (5), 826–835. https://doi.org/10.1016/j.chemosphere.2008.02.039.

Bellas, J., Nieto, O., Beiras, R., 2011. Integrative assessment of coastal pollution: development and evaluation of sediment quality criteria from chemical contamination and ecotoxicological data. Coast. Shelf Sci. 31 (5), 448–456. https://doi.org/10.1016/j.csr.2010.04.012.

Berkeley, A., Perry, C.T., Smithers, S.G., Horton, B.P., Taylor, K.G., 2007. A review of the ecological and taphonomic controls on foraminiferal assemblage development in intertidal environments. Earth Sci. Rev. 83 (3–4), 205–230. https://doi.org/10.1016/j.earscirev.2007.04.003.

Besada, V., Fumega, J., Vaamonde, A., 2002. Temporal trends of Cd, Cu, Hg, Pb and Zn in mussel (*Mytilus galloprovincialis*) from the Spanish North-Atlantic coast 1991-1999. Sci. Total Environ. 288 (3), 239–253. https://doi.org/10.1016/S0048-9697(01)01010-5.

Blythe, J., Armitage, D., Alonso, G., Campbell, D., Esteves Dias, A.C., Epstein, G., Marschke, M., Nayak, P., 2020. Frontiers in coastal well-being and ecosystem services research: a systematic review. Ocean Coast Manag. 185, 105028 https://doi.org/10.1016/j.ocecoaman.2019.105028.

Bode, A., Varela, M., 1998. Primary production and phytoplankton in three Galician Rias Altas (NW Spain): seasonal and spatial variability. Sci. Mar. 62 (4), 319–330. https://doi.org/10.3989/scimar.1998.62n4319.

Bode, A., González, N., Rodríguez, C., Varela, M., Varela, M.M., 2005. Seasonal variability of plankton blooms in the Ria de Ferrol (NW Spain): I. Nutrient concentrations and nitrogen uptake rates. Estuar. Coast Shelf Sci. 63 (1–2), 269–284. https://doi.org/10.1016/j.ecss.2004.11.020.

Borja, A., Dauer, D.M., 2008. Assessing the environmental quality status in estuarine and coastal systems: comparing methodologies and indices. Ecol. Indicat. 8 (4), 331–337. https://doi.org/10.1016/j.ecolind.2007.05.004.

Borja, A., Elliott, M., Carstensen, J., Heiskanen, A.S., van de Bund, W., 2010. Marine management – towards an integrated implementation of the European marine strategy framework and the water framework directives. Mar. Pollut. Bull. 60 (12), 2175–2186. https://doi.org/10.1016/j.marpolbul.2010.09.026.

Brennecke, D., Duarte, B., Paiva, F., Caçador, I., Canning-Clode, J., 2016. Microplastics as vector for heavy metal contamination from the marine environment. Estuar. Coast Shelf Sci. 178, 189–195. https://doi.org/10.1016/j.ecss.2015.12.003.

Brush, G.S., 2009. Historical land use, nitrogen and coastal eutrophication: a paleoecological perspective. Estuar. Coast 32, 18–28. https://doi.org/10.1007/s12237-008-9106-z.

Buceta, J.L., Lloret, A., Antequera, M., Obispo, R., Sierra, J., Martínez-Gil, M., 2015. Nuevo marco para la caracterización y clasificación del material dragado en España. Ribagua 2, 105–115. https://doi.org/10.1016/j.riba.2015.11.001.
Burgoa, J.J., 2020. Ferrol hacia el patrimonio de la humanidad. La Ilustración y el Modernismo. Central Librera, Ferrol.
Buzas-Stephens, P., Buzas, M.A., 2005. Population dynamics and dissolution of foraminifera in Nueces Bay, Texas. J. Foraminifer. Res. 35 (3), 248–258. https://doi.org/10.2113/35.3.248.
Carballeira, A., Carral, E., Puente, X., Villares, R., 1997. Estado de la conservación de la costa gallega. Universidade de Santiago de Compostela, Conselleria de Pesca, Marisqueo e Acuicultura.
Carballeira, A., Carral, E., Puente, X., Villares, R., 2000. Regional-scale monitoring of coastal contamination. Nutrients and heavy metals in estuarine sediments and organisms on the coast of Galicia (northwest Spain). Int. J. Environ. Pollut. 13, 534–572. https://doi.org/10.1504/IJEP.2000.002333.
Cardesín, J.M., 2004. 'A tale of two cities': the memory of Ferrol, between the Navy and the working class. Urban Hist. 31 (3), 329–356. https://doi.org/10.1017/S0963926805002403.
Carretero, O., Gago, J., Viñas, L., 2021. From the coast to the shelf: microplastics in Rías Baixas and Miño River shelf sediments (NW Spain). Mar. Pollut. Bull. 162, 111814 https://doi.org/10.1016/j.marpolbul.2020.111814.
Cartelle, V., García-Moreiras, I., Martínez-Carreño, N., Muñoz Sobrino, C., García-Gil, S., 2022. The role of antecedent morphology and changing sediment sources in the postglacial palaeogeographical evolution of an incised valley: the sedimentary record of the Ría de Arousa (NW Iberia). Global Planet. Change 208, 103727. https://doi.org/10.1016/j.gloplacha.2021.103727.
Cearreta, A., 1988. Distribution and ecology of benthic foraminifera in the Santoña estuary, Spain. Rev. Esp. Paleontol. 3, 23–38. https://doi.org/10.7203/sjp.25140.
Cearreta, A., Murray, J.W., 1996. Holocene paleoenvironmental and relative sea-level changes in the Santoña estuary, Spain. J. Foraminifer. Res. 26 (4), 289–299. https://doi.org/10.2113/gsjfr.26.4.289.
Cearreta, A., Irabien, M.L., Leorri, E., Yusta, I., Croudace, I.W., Cundy, A.B., 2000. Recent anthropogenic impacts on the Bilbao Estuary, Northern Spain: geochemical and microfaunal evidence. Estuar. Coast Shelf Sci. 50, 571–592. https://doi.org/10.1006/ecss.1999.0582.
Cearreta, A., Alday, M., Freitas, C., Andrade, C., Cruces, A., 2002a. Modern foraminiferal record of alternating open and restricted environmental conditions in the Santo André lagoon, SW Portugal. Hydrobiologia 475/476, 21–27. https://doi.org/10.1023/A:1020384302366.
Cearreta, A., Irabien, M.J., Leorri, E., Yusta, I., Quintanilla, A., Zabaleta, A., 2002b. Environmental transformation of the Bilbao estuary, N. Spain: microfaunal and geochemical proxies in the recent sedimentary record. Mar. Pollut. Bull. 44 (6), 487–503. https://doi.org/10.1016/S0025-326X(01)00261-2.
Cearreta, A., Alday, M., Freitas, M.C., Andrade, C., 2007. Postglacial foraminifera and paleoenvironments of the Melides Lagoon (SW Portugal): towards a regional model of coastal evolution. J. Foraminifer. Res. 37 (2), 125–135. https://doi.org/10.2113/gsjfr.37.2.125.
Cearreta, A., García-Artola, A., Leorri, E., Irabien, M.J., Masque, P., 2013. Recent environmental evolution of regenerated salt marshes in the southern Bay of Biscay: anthropogenic evidence in their sedimentary record. J. Mar. Syst. 109–110, S203–S212. https://doi.org/10.1016/j.jmarsys.2011.07.013.
Cearreta, A., Irabien, M.J., Gómez Arozamena, J.E., El bani Altuna, N., Goffard, A., García-Artola, A., 2021. Environmental evolution of the Basque Coast Geopark estuaries (southern Bay of Biscay) during the last 10,000 years. J. Mar. Syst. 219, 103557 https://doi.org/10.1016/j.jmarsys.2021.103557.
Cesbron, F., Geslin, E., Jorissen, F.J., Delgard, M.L., Charrieau, L., Deflandre, B., Jézéquel, D., Anschutz, P., Metzger, E., 2016. Vertical distribution and respiration rates of benthic foraminifera: contribution to aerobic remineralization in intertidal mudflats covered by *Zostera noltei* meadows. Estuar. Coast Shelf Sci. 179, 23–28. https://doi.org/10.1016/j.ecss.2015.12.005.
Chmura, G.L., 1994. Palynomorph distribution in marsh environments in the modern Mississippi Delta plain. GSA Bulletin 106, 705–714. https://doi.org/10.1130/0016-7606(1994)106<0705:PDIMEI>2.3.CO;2.
Cobelo-García, A., Prego, R., 2003. Heavy metal sedimentary record in a Galician Ria (NW Spain): background values and recent contamination. Mar. Pollut. Bull. 46 (10), 1253–1262. https://doi.org/10.1016/S0025-326X(03)00168-1.
Combarro, M.P., Sueiro, A., Araújo, M., Pardo, F., Garrido, M.J., 1993. Incidencia de la contaminación bacteriana en la ría de Ares-Betanzos (NW España). Microbiol. SEM 9, 14–27.
Dabrio, C.J., Zazo, C., Goy, J.L., Sierro, F.J., Borja, F., Lario, J., González, J.A., Flores, J. A., 2000. Depositional history of estuarine infill during the last postglacial transgression (Gulf of Cadiz, Southern Spain). Mar. Geol. 162 (2–4), 381–404. https://doi.org/10.1016/S0025-3227(99)00069-9.
Davis, R.A., Welty, A.T., Borrego, J., Morales, J.A., Pendon, J.G., Ryan, J.G., 2000. Rio Tinto estuary (Spain): 5000 years of pollution. Environ. Geol. 39 (10), 1107–1116. https://doi.org/10.1007/s002549900096.
Debenay, J.P., Guiral, D., Parra, M., 2002. Ecological factors acting on the microfauna in mangrove swamps. The case of foraminiferal assemblages in French Guiana. Estuar. Coast Shelf Sci. 55 (4), 509–533. https://doi.org/10.1006/ecss.2001.0906.
Debenay, J.P., Bicchi, E., Goubert, E., Armynot du Châtelet, E., 2006. Spatio-temporal distribution of benthic foraminifera in relation to estuarine dynamics (Vie estuary, Vendée, W France). Estuar. Coast Shelf Sci. 67 (1–2), 181–197. https://doi.org/10.1016/j.ecss.2005.11.014.
de Mora, S., Sheikholeslami, M.R., Wyse, E., Azemard, S., Cassi, R., 2004. An assessment of metal contamination in coastal sediments of the Caspian Sea. Mar. Pollut. Bull. 48 (1–2), 61–77. https://doi.org/10.1016/S0025-326X(03)00285-6.
de Rijk, S., Troelstra, S.R., 1997. Salt marsh foraminifera from the Great Marshes, Massachusetts: environmental controls. Palaeogeogr. Palaeoclimatol. Palaeoecol. 130 (1–4), 81–112. https://doi.org/10.1016/S0031-0182(96)00131-9.
De Witte, B., Devriese, L., Bekaert, K., Hoffman, S., Vandermeersh, G., Cooreman, K., Robbens, J., 2014. Quality assessment of the blue mussel (Mytilus edulis): comparison between commercial and wild types. Mar. Pollut. Bull. 85, 146–155. https://doi.org/10.1016/j.marpolbul.2014.06.006.
deCastro, M., Gómez-Gesteira, M., Prego, R., Taboada, J.J., Montero, P., Herbello, P., Pérez-Villar, V., 2000. Wind and tidal influence on water circulation in a Galician ria (NW Spain). Estuar. Coast Shelf Sci. 51 (2), 161–176. https://doi.org/10.1006/ecss.2000.0619.
deCastro, M., Gomez-Gesteira, M., Prego, R., Alvarez, I., 2004. Ria-ocean exchange driven by tides in the Ria of Ferrol (NW Spain). Estuar. Coast Shelf Sci. 61 (1), 15–24. https://doi.org/10.1016/j.ecss.2004.04.001.
Dessandier, P.A., Bonnin, J., Kim, J.H., Bichon, S., Grémare, A., Deflandre, B., de Stigter, H., Malaizé, B., 2015. Lateral and vertical distributions of living benthic foraminífera off the Douro River (western Iberian margin): impact of the organic matter quality. Mar. Micropaleontol. 120, 31–45. https://doi.org/10.1016/j.marmicro.2015.09.002.
Diz, P., Francés, G., Pelejero, C., Grimalt, J.O., Vilas, F., 2002. The last 3000 years in the Ría de Vigo (NW Iberian Margin): climatic and hydrographic signals. Holocene 12 (4), 459–468. https://doi.org/10.1191/0959683602hl550rp.
Diz, P., Francés, G., Costas, S., Souto, C., Alejo, I., 2004. Distribution of benthic foraminifera in coarse sediments, Ría de Vigo, NW Iberian Margin. J. Foraminifer. Res. 34 (4), 258–275. https://doi.org/10.2113/34.4.258.
Diz, P., Francés, G., Rosón, G., 2006. Effects of contrasting upwelling-downwelling on benthic foraminiferal distribution in the Ría de Vigo (NW Spain). J. Mar. Syst. 60 (1–2), 1–18. https://doi.org/10.1016/j.jmarsys.2005.11.001.
Diz, P., Francés, G., 2008. Distribution of live benthic foraminifera in the Ría de Vigo (NW Spain). Mar. Micropaleontol. 66 (3–4), 165–191. https://doi.org/10.1016/j.marmicro.2007.09.001.
Diz, P., Francés, G., 2009. Postmortem processes affecting benthic foraminiferal assemblages in the Ría de Vigo, Spain: implications for paleoenvironmental studies. J. Foraminifer. Res. 39 (3), 166–179. https://doi.org/10.2113/gsjfr.39.3.166.
Ecologistas en Acción, 2016. Informe 2016 Banderas Negras. Spain. https://www.ecologistasenaccion.org/wp-content/uploads/adjuntos-spip/pdf/informe-banderas-negras-2016.pdf.
Ellison, J.C., 2017. Applications of pollen analysis in estuarine systems. In: Weckström, K., Saunders, K.M., Gell, P.A., Skilbeck, C.G. (Eds.), Applications of Paleoenvironmental Techniques in Estuarine Studies, Developments in Paleoenvironmental Research. Springer Netherlands, Dordrecht, pp. 441–468. https://doi.org/10.1007/978-94-024-0990-1_18.
Evans, M.E., Heller, F., 2003. Environmental Magnetism. Principles and Applications of Enviromagnetics. Academic Press, United States of America.
Evans, G., Prego, R., 2003. Rias, estuaries and incised valleys: is a ria an estuary? Mar. Geol. 196, 171–175. https://doi.org/10.1016/S0025-3227(03)00048-3.
Figueiras, F.G., Labarta, U., Fernández Reiriz, M.J., 2002. Coastal upwelling, primary production and mussel growth in the Rías Baixas of Galicia. In: Vadstein, O., Olsen, Y. (Eds.), Sustainable Increase of Marine Harvesting: Fundamental Mechanisms and New Concepts. Springer Science+Business Media Dordrecht, Norway, pp. 121–131. https://doi.org/10.1007/978-94-017-3190-4_11.
Fontanier, C., Deflandre, B., Rigaud, S., Mamo, B., Dubosq, N., Lamarque, B., Langlet, D., Schmidt, S., Lebleu, P., Poirier, D., Cordier, M.A., Grémare, A., 2022. Live (stained) benthic foraminifera from the West-Gironde Mud Patch (Bay of Biscay, NE Atlantic): assessing the reliability of bio-indicators in a complex shelf sedimentary unit. Continent. Shelf Res. 232, 104616 https://doi.org/10.1016/j.csr.2021.104616.
Foucher, A., Chaboche, P.A., Sabatier, P., Evrard, O., 2021. A worldwide meta-analysis (1977-2020) of sediment core dating using fallout radionuclides including ^{137}Cs and $^{210}Pb_{xs}$. Earth Syst. Sci. Data 13, 4951–4966. https://doi.org/10.5194/essd-13-4951-2021.
Frias, J., Pagter, E., Nash, R., O'Connor, I., Carretero, O., Filgueiras, A., Viñas, L., Gago, J., Antunes, J., Bessa, F., Sobral, P., Goruppi, A., Tirelli, V., Pedrotti, M.L., Suaria, G., Aliani, S., Lopes, C., Raimundo, J., Caetano, M., Palazzo, L., de Lucia, G. A., Camedda, A., Muniategui, S., Grueiro, G., Fernandez, V., Andrade, J., Dris, R., Laforsch, C., Scholz-Böttcher, B.M., Gerdts, G., 2018. Standardised Protocol for Monitoring Microplastics in Sediments. JPI-Oceans BASEMAN project.
Gago, J., Carretero, O., Filgueiras, A.V., Viñas, L., 2018. Synthetic microfibers in the marine environment: a review on their occurrence in seawater and sediments. Mar. Pollut. Bull. 127, 365–376. https://doi.org/10.1016/j.marpolbul.2017.11.070.
García-Artola, A., Cearreta, A., Irabien, M.J., Leorri, E., Sanchez-Cabeza, J.A., Corbett, D. R., 2016. Agricultural fingerprints in salt-marsh sediments and adaptation to sea-level rise in the eastern Cantabrian coast (N. Spain). Estuar. Coast Shelf Sci. 171, 66–76. https://doi.org/10.1016/j.ecss.2016.01.031.
García-Moreiras, I., Delgado, C., Martínez-Carreño, N., García-Gil, S., Muñoz Sobrino, C., 2019. Climate and vegetation changes in coastal ecosystems during the Middle Pleniglacial and the early Holocene: two multi-proxy, high resolution records from Ría de Vigo (NW Iberia). Global Planet. Change 176, 100–122. https://doi.org/10.1016/j.gloplacha.2019.02.015.
Garmendia, J.M., Valle, M., Borja, A., Chust, G., Rodríguez, J.G., Franco, J., 2021. Estimated footprint of shellfishing activities in *Zostera noltei* meadows in a northern Spain estuary: lessons for management. Estuar. Coast Shelf Sci. 254 (5), 107320 https://doi.org/10.1016/j.ecss.2021.107320.
Goldstein, S.T., Watkins, G.T., 1999. Taphonomy of salt marsh foraminifera: an example from coastal Georgia. Palaeogeogr. Palaeoclimatol. Palaeoecol. 149 (1–4), 103–114. https://doi.org/10.1016/S0031-0182(98)00195-3.

Gómez-Orellana, L., Ramil-Rego, P., Ferreiro da Costa, J., Muñoz Sobrino, C., 2021. Holocene environmental change on the Atlantic coast of NW Iberia as inferred from the Ponzos wetland sequence. Boreas 50 (4), 1131–1145. https://doi.org/10.1111/bor.12535.

Graham, M.C., Eaves, M.A., Farmer, J.G., Dobson, J., Fallick, A.E., 2001. A study of carbon and nitrogen stable isotope and elemental ratios as potential indicators of source and fate of organic matter in sediments of the Forth Estuary. Scotland. Est. Coast. Shelf Sci. 52, 375–380. https://doi.org/10.1006/ecss.2000.0742.

Graña, J., Macías, F., 1987a. Evaluación de parámetros ambientales en la ría de Ferrol. Cuad. Marisq. Publ. Téc. 9, 223–231.

Graña, J., Macías, F., 1987b. Contaminación orgánica en las rías gallegas. Cuad. Marisq. Publ. Téc. 12, 747–752.

Greenpeace, 2005a. La calidad de las aguas en España. Un estudio por cuencas. Spain. https://archivo-es.greenpeace.org/espana/Global/espana/report/other/agua-la-calidad-de-las-aguas.pdf.

Greenpeace, 2005b. Destrucción a toda costa. Informe sobre la situación del litoral español. Spain. http://archivo-es.greenpeace.org/espana/Global/espana/report/other/destrucci-n-a-toda-costa-2005-12.pdf.

Grimm, E.C., 1987. CONISS: a FORTRAN 77 program for stratigraphically constrained cluster analysis by the method of incremental sum of squares. Comput. Geosci. 13 (1), 13–35. https://doi.org/10.1016/0098-3004(87)90022-7.

Hancock, G.J., Leslie, C., Everett, S.E., Tims, S.G., Brunskill, G.J., Haese, R., 2011. Plutonium as a chronomarker in Australian and New Zealand sediments: a comparison with ^{137}Cs. J. Environ. Radiact. 102, 919–929. https://doi.org/10.1016/j.jenvrad.2009.09.008.

Heusser, L.E., Stock, C.E., 1984. Preparation techniques for concentrating pollen from marine sediments and other sediments with low pollen density. Palynology 8 (1), 225–227. https://doi.org/10.1080/01916122.1984.9989279.

Horton, B.P., Edwards, R.J., Lloyd, J.M., 1999. UK intertidal foraminiferal distributions: implications for sea-level studies. Mar. Micropaleontol. 36 (4), 205–223. https://doi.org/10.1016/S0377-8398(99)00003-1.

Horton, B.P., Murray, J.W., 2007. The roles of elevation and salinity as primary controls on living foraminiferal distributions: cowpen Marsh, Tees Estuary, UK. Mar. Micropaleontol. 63 (3–4), 169–186. https://doi.org/10.1016/j.marmicro.2006.11.006.

Irabien, M.J., Cearreta, A., Leorri, E., Gómez, J., Viguri, J., 2008. A 130 year record of pollution in the Suances estuary (southern Bay of Biscay): implications for environmental management. Mar. Pollut. Bull. 56, 1719–1727. https://doi.org/10.1016/j.marpolbul.2008.07.006.

Irabien, M.J., Cearreta, A., Serrano, H., Villasante-Marcos, V., 2018. Environmental regeneration processes in the Anthropocene: the Bilbao estuary case (northern Spain). Mar. Pollut. Bull. 135, 977–987. https://doi.org/10.1016/j.marpolbul.2018.08.022.

Irabien, M.J., Cearreta, A., Gómez-Arozamena, J., García-Artola, A., 2020. Holocene vs Anthropocene sedimentary records in a human-altered estuary: the Pasaia case (northern Spain). Mar. Geol. 429, 106292 https://doi.org/10.1016/j.margeo.2020.106292.

Izco, J., 1987. Galicia. In: Peinado Lorca, M., Rivas Martínez, S. (Eds.), La vegetación de España. Servicio de Publicaciones Universidad de Alcalá de Henares, pp. 385–418.

Jorissen, F.J., 1987. The distribution of benthic foraminífera in the Adriatic Sea. Mar. Micropaleontol. 12, 21–48. https://doi.org/10.1016/0377-8398(87)90012-0.

Jorissen, F.J., Barmawidjaja, D.M., Puskaric, S., van der Zwaan, G.J., 1992. Vertical distribution of benthic foraminifera in the northern Adriatic Sea: the relation with the organic flux. Mar. Micropaleontol. 19, 131–146. https://doi.org/10.1016/0377-8398(92)90025-F.

Lamb, A.L., Wilson, G.P., Leng, M.J., 2006. A review of coastal palaeoclimate and relative sea-level reconstructions using δ^{13}C and C/N ratios in organic material. Earth Sci. Rev. 75, 29–57. https://doi.org/10.1016/j.earscirev.2005.10.003.

Lebreiro, S.M., Francés, G., Abrantes, F.F.G., Diz, P., Bartels-Jónsdóttir, H.B., Stroynowski, Z.N., Gil, I.M., Pena, L.D., Rodrigues, T., Jones, P.D., Nombela, M.A., Alejo, I., Briffa, K.R., Harris, I., Grimalt, J.O., 2006. Climate change and coastal hydrographic response along the Atlantic Iberian Margin (Tagus Prodelta and Muros Ría) during the last two millennia. Holocene 16 (7), 1003–1015. https://doi.org/10.1177/0959683606hl990rp.

Leorri, E., Cearreta, A., Horton, B.P., 2008. A foraminifera-based transfer function as a tool for sea-level reconstruction in the southern Bay of Biscay. Geobios 41, 787–797. https://doi.org/10.1016/j.geobios.2008.03.003.

Leorri, E., Gehrels, W.R., Horton, B.P., Fatela, F., Cearreta, A., 2010. Distribution of foraminifera in salt marshes along the Atlantic coast of SW Europe: tools to reconstruct past sea-level variations. Quat. Int. 221, 104–115. https://doi.org/10.1016/j.quaint.2009.10.033.

Loeblich, A.R., Tappan, H., 1988. Foraminiferal Genera and Their Classification. Van Nostrand Reinhold, New York.

Long, E.R., MacDonald, D.D., Smith, S.L., Calder, F.D., 1995. Incidence of adverse biological effects within ranges of chemical concentrations in marine and estuarine sediments. Environ. Manag. 19, 81–97. https://doi.org/10.1007/BF02472006.

Loubere, P., Gary, A., 1990. Taphonomic process and species microhabitats in the living to fossil assemblage transition of deeper water benthic foraminifera. Palaios 5 (4), 375–381. https://doi.org/10.2307/3514894.

Lueiro, X., Prego, R., 1999. The Ria of Ferrol: state of its knowledge. Monografías de Química Oceanográfica 1 (99), 1–30.

Mackie, E.A.V., Leng, M.J., Lloyd, J.M., Arrowsmith, C., 2005. Bulk organic δ^{13}C and C/N ratios as palaeosalinity indicators within a Scottish isolation basin. J. Quat. Sci. 20 (4), 303–312. https://doi.org/10.1002/jqs.919.

Martín García, A., 2001. El Ferrol y su tierra durante el Antiguo Régimen. Un estudio sobre población y sociedad. Obradoiro Hist. Mod. 10, 197–223.

Mateu, G., 1987. Unos datos y unas observaciones micropaleontológicas sobre las rías de Galicia. Cuaternario Geomorfol. 1, 177–194.

Mendez, G., Vilas, F., 2005. Geological antecedents of the rias Baixas (Galicia, northwest iberian Peninsula). J. Mar. Syst. 54 (1–4), 195–207. https://doi.org/10.1016/j.jmarsys.2004.07.012.

Meyers, P.A., 1997. Organic geochemical proxies of paleoceanographic, paleolimnologic and paleoclimatic processes. Org. Geochem. 27 (5–6), 213–250. https://doi.org/10.1016/S0146-6380(97)00049-1.

Miranda, D.A., Yogui, G.T., 2016. Polychlorinated biphenyls and chlorinated pesticides in king mackerel caught off the coast of Pernambuco, northeastern Brazil: occurrence, contaminant profile, biological parameters and human intake. Sci. Total Environ. 569–570 (1), 1510–1516. https://doi.org/10.1016/j.scitotenv.2016.06.241.

Mohamed, K.J., Rey, D., Rubio, B., Dekkers, M.J., Roberts, A.P., Vilas, F., 2011. Onshore-offshore gradient in reductive early diagenesis in coastal marine sediments of the Ria de Vigo, Northwest Iberian Peninsula. Continent. Shelf Res. 31 (5), 433–447. https://doi.org/10.1016/j.csr.2010.06.006.

Mojtahid, M., Jorissen, F., Pearson, T.H., 2008. Comparison of benthic foraminiferal and macrofaunal responses to organic pollution in the Firth of Clyde (Scotland). Mar. Pollut. Bull. 56 (1), 42–76. https://doi.org/10.1016/j.marpolbul.2007.08.018.

Moore, P.D., Collinson, M., Webb, J.A., 1994. Pollen Analysis. Wiley, Oxford.

Moreno, J., Valente, T., Moreno, F., Fatela, F., Guise, L., Patinha, C., 2007. Occurrence of calcareous foraminifera and calcite-carbonate equilibrium conditions – a case study in Minho/Coura estuary (Northern Portugal). Hydrobiologia 587, 177–184. https://doi.org/10.1007/s10750-007-0677-7.

Mosquera Santé, M.L., 2000. Evolución postglaciar del nivel del mar en el NO de la Península Ibérica: el caso del Golfo Ártabro. Unpublished PhD dissertation. Universidad de A Coruña, p. 186.

Muñoz Sobrino, C., Cartelle, V., Martínez-Carreño, N., Ramil-Rego, P., García Gil, S., 2022. The timing of the postglacial marine transgression in the Ría de Ferrol (NW Iberia): a new multiproxy approach from its sedimentary infill. Catena 209 (2), 105847. https://doi.org/10.1016/j.catena.2021.105847.

Murray, J.W., 1979. British Nearshore Foraminiferids, Linnean Society of London and the Estuarine and Brackish-Water Sciences Association. Academic Press London, New York, San Francisco.

Murray, J.W., 2006. Ecology and Applications of Benthic Foraminifera. Cambridge University Press, Cambridge. https://doi.org/10.1017/CBO9780511535529.

Murray, J.W., Alve, E., 1999a. Taphonomic experiments on marginal marine foraminiferal assemblages: how much ecological information is preserved? Palaeogeogr. Palaeoclimatol. Palaeoecol. 149 (1–4), 183–197. https://doi.org/10.1016/S0031-0182(98)00200-4.

Murray, J.W., Alve, E., 1999b. Natural dissolution of modern shallow water benthic foraminifera: taphonomic effects on the palaeoecological record. Palaeogeogr. Palaeoclimatol. Palaeoecol. 146 (1–4), 195–209. https://doi.org/10.1016/S0031-0182(98)00132-1.

Murray, J.W., Alve, E., 2000. Major aspects of foraminiferal variability (standing crop and biomass) on a monthly scale in an intertidal zone. J. Foraminifer. Res. 30 (3), 177–191. https://doi.org/10.2113/0300177.

Nayar, S., Goh, B.P.L., Chou, L.M., Reddy, S., 2003. In situ microcosms to study the impact of heavy metals resuspended by dredging on periphyton in a tropical estuary. Aquat. Toxicol. 64, 293–306. https://doi.org/10.1016/S0166-445X(03)00062-6.

Newton, A., Icely, J., Cristina, S., Brito, A., Cardoso, A.C., Colijn, F., Riva, S.D., Gertz, F., Hansen, J.W., Holmer, M., Ivanova, K., Lekppäkoski, E., Canu, D.M., Mocenni, C., Mudge, S., Murray, N., Pejrup, M., Razinkovas, A., Reizopoulou, S., Pérez-Ruzafa, A., Schernewski, G., Schubert, H., Carr, L., Solidoro, C., Viaroli, P.L., Zaldívar, J.M., 2014. An overview of ecological status, vulnerability and future perspectives of European large shallow, semi-enclosed coastal systems, lagoons and transitional waters. Estuar. Coast Shelf Sci. 140 (1), 95–122. https://doi.org/10.1016/j.ecss.2013.05.023.

O'Flanagan, P., 2008. Port ities of Atlantic Iberia, C. 1500-1900. Ashgate, Aldershot.

Ospina-Alvarez, N., Prego, R., Álvarez, I., deCastro, M., Álvarez-Ossorio, M.T., Pazos, Y., Campos, M.J., Bernárdez, P., Garcia-Soto, C., Gómez-Gesteira, M., Varela, M., 2010. Oceanographical patterns during a summer upwelling-downwelling evento in the northern Galician rias: comparison with the whole ria system (NW of iberian Peninsula). Continent. Shelf Res. 30 (12), 1362–1372. https://doi.org/10.1016/j.csr.2010.04.018.

Otero, X.L., Vidal-Torrado, P., Calvo de Anta, R.M., Macías, F., 2005. Trace elements in biodeposits and sediments from mussel culture in the Ría de Arousa (Galicia, NW Spain). Environ. Pollut. 136 (1), 119–134. https://doi.org/10.1016/j.envpol.2004.11.026.

Otero, X.L., Calvo de Anta, R.M., Macías, F., 2009. Iron geochemistry under mussel rafts in the Galician ria system (Galicia-NW Spain). Estuar. Coast Shelf Sci. 81 (1), 83–93. https://doi.org/10.1016/j.ecss.2008.10.006.

Pan, K., Wang, W.X., 2012. Trace metal contamination in estuarine and coastal environments in China. Sci. Total Environ. 421–422, 3–16. https://doi.org/10.1016/j.scitotenv.2011.03.013.

Pascual, A., Martínez-García, B., Mendicoa, J., 2019. Benthic foraminifers as a proxy of the range of the tidal wave in the Oyambre Estuary (Cantabria, Spain). Continent. Shelf Res. 176, 1–18. https://doi.org/10.1016/j.csr.2019.02.008.

Penaud, A., Ganne, A., Eynaud, F., Lambert, C., Coste, P.O., Herlédan, M., Vidal, M., Goslin, J., Stéphan, P., Charria, G., Pailler, Y., Durand, M., Zumaque, J., Mojtahid, M., 2020. Oceanic *versus* continental influences over the last 7kyrs from a mid-shelf record in the northern Bay of Biscay (NE Atlantic). Quat. Sci. Rev. 229, 106135 https://doi.org/10.1016/j.quascirev.2019.106135.

Pérez, A., Escobedo, R., Castro, R., Jesus, R., Cardich, J., Romero, P.E., Salas-Gismondi, R., Ochoa, D., Aponte, H., Sanders, C.J., Carré, M., 2022. Carbon and

nutrient burial within Peruvian coastal marsh driven by anthropogenic activities. Mar. Pollut. Bull. 181, 113948 https://doi.org/10.1016/j.marpolbul.2022.113948.
Pérez Alberti, A., Rodríguez, X., Graña, J., Máiz, B., Cristobo, F.J., Urgorri, V., Lamas, A., Rodríguez-Villasante, J.A., 2002. Ría de Ferrol. A Perla Ártabra. Cadernos Ateneo Ferrolán, Ferrol.
Perry, C.T., Berkeley, A., Smithers, S.G., 2008. Microfacies characteristics of a tropical, mangrove-fringed shoreline, Cleveland Bay, Queensland, Australi: sedimentary and taphonomic controls on mangrove facies development. J. Sediment. Res. 78 (2), 77–97. https://doi.org/10.2110/jsr.2008.015.
Phuong, N.N., Poirier, L., Lagarde, F., Kamari, A., Zalouk-Vergnoux, A., 2018. Microplastic abundance and characteristics in French Atlantic coastal sediments using a new extraction method. Environ. Pollut. 243 (A), 228–237. https://doi.org/10.1016/j.envpol.2018.08.032.
Pirrie, D., Power, M.R., Rollinson, G., Camm, G.S., Hughes, S.H., Butcher, A.R., Hughes, P., 2003. The spatial distribution and source of arsenic, copper, tin and zinc within the surface sediments of the Fal Estuary, Cornwall, UK. Sedimentology 50, 579–595. https://doi.org/10.1046/j.1365-3091.2003.00566.x.
Planelles de Miguel, P., 1996. Foraminíferos bentónicos actuales de sustratos blandos intermareales de la Ría de Ferrol (Galicia). Estudio faunístico y autoecológico. Unpublished PhD dissertation. Universidad de Santiago de Compostela, p. 580.
Prego, R., Varela, M., 1998. Hydrography of the Artabro Gulf in summer: western coastal limit of Cantabrian seawater and wind-induced upwelling at prior cape. Oceanol. Acta 21 (2), 145–155. https://doi.org/10.1016/S0399-1784(98)80004-2.
Prego, R., Barciela, M.C., Varela, M., 1999. Nutrient dynamics in the Galician coastal area (northwestern iberian peninula): do the rias bajas receive more nutrient salts than the rias altas? Continent. Shelf Res. 19 (3), 317–334. https://doi.org/10.1016/S0278-4343(98)00099-5.
Prego, R., Cobelo-García, A., 2003. Twentieth century overview of heavy metals in the Galician Rias (NW Iberian Peninsula). Environ. Pollut. 121 (3), 425–452. https://doi.org/10.1016/S0269-7491(02)00231-2.
Reaves, C.M., 1986. Organic matter metabolizability and calcium carbonate dissolution in nearshore marine muds. J. Sediment. Res. 56 (4), 486–494. https://doi.org/10.1306/212F8963-2B24-11D7-8648000102C1865D.
Reille, M., 1992. Pollen et spores d'Europe et d'Afrique du Nord. Laboratoire de Botanique historique et Palynologie, Marseille.
Rial, D., León, V.M., Bellas, J., 2017. Integrative assessment of coastal marine pollution in the Bay of santander and the upper Galician rias. J. Sea Res. 130, 239–247. https://doi.org/10.1016/j.seares.2017.03.006.
Rico Boquete, E., 1995. El rechazo de una opción conservacionista e integradora. Galicia en el Plan General de Repoblación Forestal de España de 1939. Not. Hist. Agrar. 9, 155–173.
Rodil, R., Villaverde-de-Sáa, E., Cobas, J., Quintana, J.B., Cela, R., 2019. Legacy and emerging pollutants in marine bivalves from the Galician coast (NW Spain). Environ. Int. 129, 364–375. https://doi.org/10.1016/j.envint.2019.05.018.
Rodríguez-Lázaro, J., Pascual, A., Martínez-García, B., 2013. Recent benthic foraminifers as indicators of the sedimentary dynamics of the Tina Mayor and Tina Menor estuaries (S Bay of Biscay, N Spain). J. Mar. Syst. 109–110 (Suppl. ment), S213–S232. https://doi.org/10.1016/j.jmarsys.2012.04.005.
Ruiz, F., Borrego, J., González-Regalado, M.L., López González, N., Carro, B., Abad, M., 2008. Impact of millennial mining activities on sediments and microfauna of the Tinto River estuary (SW Spain). Mar. Pollut. Bull. 56 (7), 1258–1264. https://doi.org/10.1016/j.marpolbul.2008.04.036.
Sanders, D., 2003. Syndepositional dissolution of calcium carbonate in neritic carbonate environments: geological recognition, processes, potential significance. J. Afr. Earth Sci. 36 (3), 99–134. https://doi.org/10.1016/S0899-5362(03)00027-7.
Santos, L., Bao, R., Sánchez Goñi, M.F., 2001. Pollen record of the last 500 years from the Doninos Coastal Lagoon (NW Iberian Peninsula): changes in the pollinic catchment size versus paleoecological interpretation. J. Coast Res. 17 (3), 705–713.
Santos, R.A., Ledru, M.P., 2021. Acid-free protocol for extracting pollen from Quaternary sediments. Palynology 46 (1), 1–8. https://doi.org/10.1080/01916122.2021.1960916.
Scott, D.B., Medioli, F.S., Schafer, C.T., 2007. Monitoring in Coastal Environments Using Foraminifera and Thecamoebian Indicators. Cambridge University Press, Cambridge. https://doi.org/10.1017/CBO9780511546020.
Scott, G., Thompson, L., Hitchin, R., Scourse, J., 1998. Observations on selected salt-marsh and shallow-marine species of agglutinating foraminifera: grain size and mineralogical selectivity. J. Foraminifer. Res. 28 (4), 261–267. https://doi.org/10.2113/gsjfr.28.4.261.
Serrano, H., 2020. El registro sedimentario Antropoceno de los ecosistemas costeros cantábricos. Procesos de regeneración ambiental en los estuarios del Saja-Besaya (Cantabria) y del Nervión (Bizkaia). Unpublished PhD dissertation. Universidad del País Vasco UPV/EHU, p. 291.
Surís-Regueiro, J.C., Santiago, J.L., 2014. Characterization of fisheries dependence in Galicia (Spain). Mar. Pol. 47, 99–109. https://doi.org/10.1016/j.marpol.2014.02.006.
Teichert, N., Borja, A., Chust, G., Uriarte, A., Lepage, M., 2016. Restoring fish ecological quality in estuaries: implication of interactive and cumulative effects among anthropogenic stressors. Sci. Total Environ. 542 A (15), 383–393. https://doi.org/10.1016/j.scitotenv.2015.10.068.
Valente, T., Fatela, F., Moreno, J., Moreno, F., Guise, L., Patinha, C., 2009. A comparative study of the influence of geochemical parameters on the distribution of foraminiferal assemblages in two distinctive tidal marshes. J. Coast. Res. SI 56, 1439–1443.
Van Voorthuysen, J.H., 1973. Foraminiferal ecology in the ria de Arosa, Galicia, Spain. Zool. Verhandel. 123, 1–68.
Vane, C.H., Jones, D.G., Lister, T.R., 2009. Mercury contamination in surface sediments and sediment cores of the Mersey Estuary, UK. Mar. Pollut. Bull. 58 (6), 940–946. https://doi.org/10.1016/j.marpolbul.2009.03.006.
Varela, M.M., Bode, A., González, N., Rodríguez, C., Varela, M., 2003. Fate of organic matter in the Ría of Ferrol (Galicia, NW Spain): uptake by pelagic bacteria vs. particle sedimentation. Acta Oecol. 24 (1), S77–S86. https://doi.org/10.1016/S1146-609X(03)00015-8.
Vilas, F., Bernabéu, A., Rubio, B., Rey, D., 2018. The Galician rías. NW coast of Spain. In: Morales, J.A. (Ed.), The Spanish Coastal Systems. Springer, Switzerland, pp. 387–414. https://doi.org/10.1007/978-3-319-93169-2_17.
Walker, S.E., Goldstein, S., 1999. Taphonomic tiering: experimental field taphonomy of molluscs and foraminifera above and below the sediment-water interface. Palaeogeogr. Palaeoclimatol. Palaeoecol. 149 (1–4), 227–244. https://doi.org/10.1016/S0031-0182(98)00203-X.
Walton, W.R., 1952. Techniques for recognition of living foraminifera. Contrib. Cushman Found. Foraminifer. Res. 3, 56–60.
Zalasiewicz, J., Waters, C.N., Ivar do Sul, J.A., Corcoran, P.L., Barnosky, A.D., Cearreta, A., Edgeworth, M., Gałuszka, A., Jeandel, C., Leinfelder, R., McNeill, J.R., Steffen, W., Summerhayes, C., Wagreich, M., Williams, M., Wolfe, A.P., Yonan, Y., 2016. The geological cycle of plastics and their use as a stratigraphic indicator of the Anthropocene. Anthropocene 13, 4–17. https://doi.org/10.1016/j.ancene.2016.01.002.